Cumulate formation and melt extraction from mush-dominated magma reservoirs: the melt flush process exemplified at mid-ocean ridges

Marine Boulanger, Lydéric France

▶ **To cite this version:**

Marine Boulanger, Lydéric France. Cumulate formation and melt extraction from mush-dominated magma reservoirs: the melt flush process exemplified at mid-ocean ridges. Journal of Petrology, 2023, 64, 10.1093/petrology/egad005 . hal-04009717

HAL Id: hal-04009717

https://uca.hal.science/hal-04009717v1

Submitted on 1 Mar 2023

HAL is a multi-disciplinary open access archive for the deposit and dissemination of scientific research documents, whether they are published or not. The documents may come from teaching and research institutions in France or abroad, or from public or private research centers.

L'archive ouverte pluridisciplinaire **HAL**, est destinée au dépôt et à la diffusion de documents scientifiques de niveau recherche, publiés ou non, émanant des établissements d'enseignement et de recherche français ou étrangers, des laboratoires publics ou privés.

Cumulate formation and melt extraction from mush-dominated magma reservoirs: the melt flush process exemplified at mid-ocean ridges

Marine Boulanger[1, 2]

Lydéric France[1,3]

[1]Université de Lorraine, CNRS, CRPG, F-54000 Nancy, France

[2]Laboratoire Magmas et Volcans, CNRS-OPGC-IRD, Université Clermont Auvergne, France

[3]Institut Universitaire de France (IUF), France

*Corresponding author: Marine Boulanger marine.boulanger@uca.fr

Keywords: Igneous cumulate, crystal mushes, reactive porous flow, assimilation-fractional crystallization, oceanic crust

© The Author(s) 2023. Published by Oxford University Press. All rights reserved. For Permissions, please email: journals.permissions@oup.com

ORIGINAL UNEDITED MANUSCRIPT

Downloaded from https://academic.oup.com/petrology/advance-article/doi/10.1093/petrology/egad005/6998539 by guest on 13 February 2023

ABSTRACT

Volcanism is the surface expression of extensive magmatic systems, with their intrusive counterpart representing ~80% of the total magma budget. Our knowledge of igneous processes therefore largely relies on our understanding of deep plutonic processes. In continental or oceanic environments, most of the intrusive igneous rocks bear geochemical cumulate signatures (e.g., depletion in incompatible elements and enrichment in compatible ones) that are commonly explained by mineral-melt segregation during differentiation. Deformation-assisted compaction aided by melt buoyancy is usually referred to as the main process involved in melt extraction. However, buoyancy alone is not sufficient, and a number of cumulative rocks are lacking any compaction evidence, opening the potential for the involvement of other processes. In addition, our view of magmatic systems has shifted in the last decades from large melt-rich bodies to crystal-rich magma reservoirs. This paradigm shift challenges some of the long-established first-order igneous concepts like the idea that melt differentiation at depth is mainly governed by (fractional) crystallization; alternatively, the presence of mush potentially favors additional processes such as melt-mush reactions.

We propose a novel igneous process for the formation of igneous cumulates, consistent with the mushy nature of oceanic igneous reservoirs, their continuous/cyclic replenishment by primitive melts, and the widespread occurrence of reactive porous flow (RPF) during magma differentiation identified in a growing number of magmatic systems. The "*melt flush*" process relies on melt-mush reactions between the primitive recharge melt(s) and crystal mush. Replacement of the more evolved interstitial melt by the primitive recharge melt leading to reactions (dissolution+crystallization), and concomitant extraction of the more evolved melt from the cumulate by buoyancy participate in the acquisition of the final cumulate signature.

ORIGINAL UNEDITED MANUSCRIPT

Downloaded from https://academic.oup.com/petrology/advance-article/doi/10.1093/petrology/egad005/6998539 by guest on 13 February 2023

This process relying on oceanic igneous systems considers for the first time melt inputs and not only melt extraction, and matches the petrographic (e.g., mineral dissolution evidence) and geochemical constraints (trace element signatures) brought by natural oceanic samples. We tested various melt-mush reactions likely involved in the early stages of the *melt flush* process during RPF to investigate their thermodynamic feasibility with the Magma Chamber Simulator. First-order results show that one-step equilibration of primitive melts with primitive to moderately differentiated mush crystals triggers mineral assimilation. Together with the constraints established from the natural rock record, it strengthens the idea that RPF is a potential key process for magma differentiation in magma reservoirs at different evolution stages. The proposed *melt flush* process eventually adds to other processes involved in cumulate formation like magma compaction or crystal settling, and is likely to apply to any other magmatic system from various settings sharing similar reservoir characteristics.

INTRODUCTION

In both continental and oceanic settings, magma reservoir formation is the consequence of the cyclic injection of primitive melts from the mantle into the crust (e.g., Annen *et al.*, 2006, 2015; Rannou *et al.*, 2006; Godard *et al.*, 2009; Cordier *et al.*, 2010; Cashman *et al.*, 2017; Sparks *et al.*, 2019; Boulanger *et al.*, 2020). Melt differentiation paths within reservoirs, hence their evolution, are a function of several parameters such as the primitive melt composition and flux, the physical conditions of crystallization (e.g., pressure, fO_2), or the reservoir architecture and thermal state and evolution. The physical behavior of a magma *sensu lato* depends largely on its crystal load (Costa *et al.*, 2009; Cashman *et al.*, 2017), and we will hereafter consider that a magma *sensu stricto* is an unlocked system where the crystal load allows magma migration, whereas a mush is locked, and cannot be mobilized for extensive mush migration and potential eruption without involving, for example, a

ORIGINAL UNEDITED MANUSCRIPT

Downloaded from https://academic.oup.com/petrology/advance-article/doi/10.1093/petrology/egad005/6998539 by guest on 13 February 2023

rejuvenation episode, tectonic events, second boiling, etc (e.g., Tait et al., 1989; Woods and Cardoso, 1997; Bachmann and Bergantz, 2003; Till et al., 2015; Seropian et al., 2021). Although still controversial (e.g., Latypov *et al.*, 2020), most current models of crustal reservoirs describe mush-dominated environments (Cashman *et al.*, 2017; Bachmann and Huber, 2019; Lissenberg *et al.*, 2019; Sparks *et al.*, 2019). Melt emplacement and migration mechanisms, and the efficiency and timing of melt extraction are dictated by the medium (melt viscosity and density, and crystal load fraction) that contains within a mush only a few volume percent of liquid within a crystal framework (Lejeune and Richet, 1995; Vigneresse *et al.*, 1996; Cheadle *et al.*, 2004; Costa *et al.*, 2009). In general, the magma-to-mush transition is attained between 40 and 60% crystals (e.g., Mainprice, 1997; Cashman *et al.*, 2017) and depends on the shape of the mush forming minerals. The exact amount of melt in the reservoirs is difficult to determine (Paulatto et al., 2022) but is likely variable, as imaged seismically and with other geophysical methods (Singh *et al.*, 1998; Zandt *et al.*, 2003; Canales *et al.*, 2009, 2017; Desissa *et al.*, 2013; Comeau *et al.*, 2015; Dunn, 2015; Magee *et al.*, 2018; Laumonier *et al.*, 2019 and references therein). Magma dynamics, in turn, control the processes operating during melt differentiation (e.g. Meurer and Boudreau, 1989a; Picard *et al.*, 2011; Leuthold *et al.*, 2014; Lissenberg and MacLeod, 2016; Boulanger *et al.*, 2020, 2021; Ferrando *et al.*, 2021a): crystallization could proceed at equilibrium, be fractionated or involve in situ crystallization (Langmuir, 1989), melt eventually could be trapped or segregated, and disequilibrium interactions between the melt and their surroundings could potentially occur (e.g. Spera and Bohrson, 2004; see definitions in Box 1). The latter tend to be of particular interest when considering mush-dominated magma reservoirs, and reactive porous flow (RPF) appears to be likely widespread and critical to melt differentiation in oceanic and potentially continental environments (Lissenberg and Dick, 2008; Cooper *et al.*, 2016; Jackson *et al.*, 2018; Hepworth *et al.*, 2020).

ORIGINAL UNEDITED MANUSCRIPT

Downloaded from https://academic.oup.com/petrology/advance-article/doi/10.1093/petrology/egad005/6998539 by guest on 13 February 2023

The textures and the geochemical signatures of igneous rocks are commonly used to identify and quantify the differentiation processes that take place during their formation. One key signature is the cumulate character of many plutonic lithologies, which were historically interpreted as evidence for crystal-melt segregation and melt differentiation by fractional crystallization (FC) and deformation (Bowen, 1915, 1920; Irvine, 1982). Here, we examine the recent petrological and geophysical developments and the latest architecture models of igneous plumbing systems, together with an overview of the different models of melt-mush reactions and reactive porous flow that have been developed in various settings. We particularly focus on oceanic magma reservoirs where the study of these processes is most advanced. Together with a new test of the thermodynamic feasibility of characteristic melt-mush reactions, we examine in light of all these elements the potential impact of RPF on the development of cumulate geochemical signatures in magma reservoirs. We suggest the involvement of a novel integrated igneous process: the *melt flush* process. We finally discuss the potential for the application of this process to magmatic systems from other geodynamic settings.

CUMULATE FORMATION PROCESSES

Processes and limitations

The term cumulate was first proposed by Wager *et al.* (1960) and referred to igneous rocks formed by crystal accumulation. In this case, the formation of cumulates involves crystal segregation and FC, as previously described by Bowen (1915). The removal of the most evolved melt fraction from cumulate minerals results in whole-rock compositions that are characteristically depleted in incompatible trace elements compared to the primitive melt composition (e.g., with a positive Eu anomaly if the cumulate assemblage includes plagioclase; Fig. 1; Meurer and Boudreau, 1989a). The main processes considered for crystal

ORIGINAL UNEDITED MANUSCRIPT

Downloaded from https://academic.oup.com/petrology/advance-article/doi/10.1093/petrology/egad005/6998539 by guest on 13 February 2023

accumulation and melt extraction are linked to melt buoyancy and gravitationally-driven viscous compaction (e.g., Mckenzie, 1984; Meurer and Boudreau, 1989b; Holness *et al.*, 2017b; Lissenberg *et al.*, 2019), the latter of which can be assisted by tectonic stresses (e.g.; Bowen, 1920; Kohlstedt and Holtzman, 2009; Holness *et al.*, 2017b; Lissenberg *et al.*, 2019; Zhang *et al.*, 2020). Cumulates can also form by compositional convection that is governed by the density contrast between intercumulus melts and an overlying magma chamber melt, without involving complete physical separation of intercumulus melts from crystals and without considering melt-mush reactions (Tait et al., 1984; Toplis et al., 2008; Namur and Charlier, 2012). However, the efficiency of these processes in the lower crust has been challenged, especially in mushy systems in the absence of any large magma chamber (Holness, 2018; Krättli and Schmidt, 2021). Buoyancy alone is likely insufficient for efficient and rapid crystal-melt segregation in mushes where the melt flux is resisted by the strength of the crystal matrix and the viscosity of the percolating melt (Daines and Pec, 2015; Bachmann and Huber, 2019). Basaltic and picritic melts with low viscosities have more potential for segregation, yet the thickness of the mush layer is critical and additional concurrent processes are required for small (~100 m-scale) systems (*Daines and Pec, 2015*). Viscous compaction is favored in reservoirs with thick mush columns subject to low cooling rates and comprising relatively dense crystallizing mineral assemblages such as mafic systems (e.g., Holness *et al.*, 2017b; Lissenberg *et al.*, 2019), although the lack of textural evidence such as intracrystalline deformation in many mafic cumulates from continental and oceanic settings questions the importance of this process (Cheadle and Gee, 2017; Holness *et al.*, 2017b; Holness, 2018; Ferrando *et al.*, 2021a). An alternative process is crystal repacking or mechanical compaction by grain rearrangement (e.g., Holness *et al.*, 2017b; Bachmann and Huber, 2019, and references therein). The efficiency of the process is constrained to a limited crystallinity range, yet the amount of melt extracted is potentially significant depending on the

ORIGINAL UNEDITED MANUSCRIPT

Downloaded from https://academic.oup.com/petrology/advance-article/doi/10.1093/petrology/egad005/6998539 by guest on 13 February 2023

morphology of the minerals (Bachmann and Huber, 2019). Crystal repacking is caused at the reservoir scale by differential stresses generated by processes such as recharge or tectonic forces, and is likely to lead to the development of a crystal fabric or to be accompanied by dissolution-precipitation aiding compaction without crystal deformation (Holness *et al.*, 2017b; Bachmann and Huber, 2019). Alternatively, gas or fluid percolation through the melt can aid its extraction from the (here passive) crystal matrix (Boudreau, 2016; Bachmann and Huber, 2019). The models detailed above only consider melt extraction from the systems and do not consider the potential impact of recharge melts migrating within the crystal mush from lower levels, as currently suggested for magma reservoirs in different settings (e.g., Jackson *et al.*, 2018; Dick *et al.*, 2019). Hence, most of these models do not consider any primitive melt inputs and, when occurring, the potential crystal-melt disequilibrium and the impact RPF to the formation of rocks bearing geochemical cumulate signatures.

Implications for melt extraction

In addition to their implications for cumulate formation, processes associated with melt migration and segregation in magma reservoirs are key to a better understanding of the volcanic-plutonic connection, which is the link between extracted melts, involved in the genesis of erupted magmas, and their crystal-rich reservoirs that ultimately cool to form plutons (e.g., Bachmann *et al.*, 2007; Schaen *et al.*, 2021). For example, the modes of extraction of large volumes of crystal-poor magma from silicic crystal mushes are critical to comprehend the dynamics of large continental volcanic systems (100 to 1000 km^3), their mobilization to produce eruption, and related monitoring. Yet, as shown in the above section they remain controversial for both silica-rich an silica-poor systems, especially regarding the efficiency and timescales of melt extraction (e.g., Bachmann and Bergantz, 2004; Burgisser and Bergantz, 2011; Holness, 2018; Bachmann and Huber, 2019; Sparks *et al.*, 2019). On

ORIGINAL UNEDITED MANUSCRIPT

Downloaded from https://academic.oup.com/petrology/advance-article/doi/10.1093/petrology/egad005/6998539 by guest on 13 February 2023

another scale, mid-ocean ridge basalts (MORBs) and related products are often studied for their interest in constraining the mantle compositions and heterogeneities, taking into account potential processes occurring between mantle melting and eruption (e.g., Rubin *et al.*, 2009; O'Neill and Jenner, 2012; Lambart *et al.*, 2019; Neave *et al.*, 2019). These processes depend on the volumes and fluxes of melts emplaced within the crust that in turn control the magma reservoir's structure, thermal architecture, composition, and evolution (e.g., Dunn *et al.*, 2005; Coogan, 2014; Dunn, 2015; Chen *et al.*, 2021). MORBs, especially at slow-spreading ridges, record geochemical signatures consistent with an evolution of melts by RPF or assimilation of gabbroic lithologies, which is also supported by textural evidence for assimilation recorded in crustal gabbros (e.g., Lissenberg and Dick, 2008; Lissenberg *et al.*, 2013; Lissenberg and MacLeod, 2016; Leuthold *et al.*, 2018; Shimizu *et al.*, 2019; Boulanger *et al.*, 2020; Sanfilippo *et al.*, 2020). This suggests that significant volumes of reacted melts can segregate from high-crystallinity mushes where RPF might occur, yet this segregation is still a matter of debate. However, olivine gabbro cumulates from a magmatic crustal section drilled at the Atlantis Bank oceanic core complex (OCC; IODP hole U1473A, Southwest Indian Ridge; SWIR) present recurrent fine-grained domains also found in other crustal sections (Bloomer et al., 1991). They are interpreted as areas of interstitial reactive melts collection from the crystal mush, supporting the melt segregation hypothesis (Ferrando *et al.*, 2021a).

EVOLUTION OF OCEANIC IGNEOUS RESERVOIRS

Impact of reactive porous flow

Magma reservoirs at oceanic spreading ridges were long suspected to be mush-dominated environments (e.g., Sinton and Detrick, 1992), a reservoir structuring with strong implications on the differentiation path of magmas. Indeed, heterogeneous modal proportions and mineral compositions observed at all scales in the oceanic crust suggest that melts are

ORIGINAL UNEDITED MANUSCRIPT

Downloaded from https://academic.oup.com/petrology/advance-article/doi/10.1093/petrology/egad005/6998539 by guest on 13 February 2023

unlikely to maintain local chemical equilibrium with the crystal framework through which they percolate, and rather interact with it (Lissenberg *et al.*, 2019; Yang *et al.*, 2019). Providing sufficient melt flux, protracted interactions with (or assimilation of) the crystal framework could ultimately result in a state of equilibrium and homogenization of the system (Blundy, 2022). Several studies have proposed the ubiquitous involvement of RPF and its strong control on the melt and crystal compositions. It has been suggested either at the mineral scale (Sanfilippo *et al.*, 2020), the scale of a mush column (Ferrando *et al.*, 2021a), the scale of a magma reservoir (Boulanger *et al.*, 2020), or the scale of the entire crustal section (Zhang *et al.*, 2020) drilled at the Atlantis Bank OCC (Dick *et al.*, 2000, 2019). These results are in agreement with previous studies conducted at Atlantis Bank and other spreading ridges, which predicted the strong control of RPF on the lithologies and differentiating melt composition (e.g., Coogan *et al.*, 2000; Kvassnes, 2004; Gao *et al.*, 2007; Lissenberg and Dick, 2008; Lissenberg and MacLeod, 2016; Ferrando *et al.*, 2018; Leuthold *et al.*, 2018; Lissenberg *et al.*, 2019, and references therein). In detail, two main lines of evidence support the RPF hypothesis (see Table 1). First, the gabbro cumulates (*sensu lato*; Fig. 1) present modal compositions that usually deviate from the typical thermodynamically constrained tholeiitic liquid line of descent (e.g., Dick *et al.*, 2019; Boulanger *et al.*, 2020). The gabbro cumulates also present minerals with characteristic textures that, despite the strong heterogeneity described in all crustal sections and oceanic crust samples, can be found on a recurrent basis. Olivine (Ol) textures are often characterized by round shapes (Fig. 2f, k, r), especially Ol chadacrysts engulfed in poikilitic plagioclase (Pl) or clinopyroxene (Cpx, Fig. 2b, f, o), or irregular and wavy contacts with surrounding minerals suggesting resorption of the grains (Fig. 2d, i). Pl present very irregular grain boundaries that often crosscut the twins of the grain with dissolution fronts (Fig. 2j), and are found as chadacrysts in both Pl (Fig. 2n) or Cpx oikocrysts (Fig. 2c, e, f, h, m, p). They can also present complex zoning patterns,

ORIGINAL UNEDITED MANUSCRIPT

Downloaded from https://academic.oup.com/petrology/advance-article/doi/10.1093/petrology/egad005/6998539 by guest on 13 February 2023

reversed or normal, with resorbed core remnants (Fig. 2g, i). The first Cpx textures that were associated with RPF are the large (sometimes pegmatitic) poikilitic grains that contain numerous Ol and/or Pl chadacrysts with resorbed grain boundaries (Fig. 2e). Cpx-Amphibole symplectites (or Cpx-Orthopyroxene symplectites) are regularly found in oceanic samples but their RPF origin is debated (Fig. 2a, h). In addition to symplectites, Cpx-Cpx intergrowths are also frequently found in samples presenting other RPF textures, and are suspected to result from this process (Fig. 2a, j, l; summary available in Table 1; e.g., Lissenberg and Dick, 2008; Lissenberg *et al.*, 2013; Sanfilippo *et al.*, 2015; Lissenberg and MacLeod, 2016; Leuthold *et al.*, 2018; Boulanger *et al.*, 2020; Zhang *et al.*, 2020; Ferrando *et al.*, 2021b). However, the disequilibrium reactions can also be more cryptic and the second line of evidence, the in situ mineral compositions, is also critical to identify the occurrence of RPF within the systems (Lissenberg and MacLeod, 2016; Sanfilippo *et al.*, 2020). There are two main components to the RPF geochemical signatures, initially described as enrichments in incompatible elements compared to the compositions expected after simple crystallization. First, the incompatible trace element contents of minerals from various gabbroic rocks are indeed higher than expected for their corresponding major element contents, which characterizes a decoupling between major and trace elements observed in the natural samples. For example, TiO_2 contents in Cpx reaches up to 1.5 wt% in minerals at very high Mg# of about 90 (Boulanger et al., 2020), or the range of La contents is the same for Pl with An contents ranging between 45 and 85. This decoupling is likely due to the progressive enrichment in incompatible trace elements with concomitant major element reequilibration of the melt with the crystal framework during RPF (e.g., towards higher Mg# for Cpx during percolation of Ol-rich crystal frameworks). The second characteristic signature is the strong fractionation between trace elements with variable degrees of incompatibility that has only been reconciled so far with an evolution modelled by AFC (DePaolo, 1981; Fig. 3A). Other processes likely to occur

ORIGINAL UNEDITED MANUSCRIPT

Downloaded from https://academic.oup.com/petrology/advance-article/doi/10.1093/petrology/egad005/6998539 by guest on 13 February 2023

in oceanic systems have failed to reproduce these signatures (e.g., Sanfilippo *et al.*, 2020; Boulanger *et al.*, 2021; Ferrando *et al.*, 2021b). Equilibrium or FC do not lead to the formation of assimilation textures, and completely fail to explain the fractionation of the incompatible trace elements of the minerals. Trapped melt crystallization was first mentioned to be the cause of the trace element enrichments in a variety of samples (Ross and Elthon, 1997; Borghini and Rampone, 2007), yet the process by itself cannot be the cause for the assimilation textures, systematic normal zoning of minerals is lacking in many samples, in addition to accessory phases that should result from trapped melt crystallization. Finally, trapped melt alone cannot account for the significant decoupling between major and trace elements observed in samples, nor for the fractionation between incompatible trace elements (especially REE) with different degrees of incompatibility found in most natural samples (Sanfilippo et al., 2020; Boulanger et al., 2021; Ferrando et al., 2021b). Additional effects of sub-solidus diffusion on the geochemical signatures, or associated with variations of the temperature-dependent partition coefficients of trace elements during the processes mentioned before also do not sufficiently impact the signatures to account for the observed natural sample record, nor explain the assimilated textures (Sanfilippo et al., 2020). Instead, these signatures tend to be interpreted as resulting from RPF with the support of the textural evidence found in the same sample (summarized in Table 1). Fig. 4 presents the comparison between Pl, Cpx and MORB compositions from various fast-spreading (FSR) and slow-spreading (SSR) ridges, and geochemical models of FC and AFC for incompatible rare earth elements (REE). It shows that FC fells short to explain the range of compositions of these systems, and that the potential impact of RPF (modeled here by AFC) on incompatible elements is found in all components of the oceanic crust and may significantly impact oceanic crustal accretion. The incompatible element contents of Pl and Cpx seem to require both the assimilation of Ol and/or Pl, but they do not record the same crystallization events. While

ORIGINAL UNEDITED MANUSCRIPT

Downloaded from https://academic.oup.com/petrology/advance-article/doi/10.1093/petrology/egad005/6998539 by guest on 13 February 2023

crystallization of Cpx help reproduce de composition of Pl, Ol crystallization help reproduce the composition of Cpx (Fig. 4). This effect is likely the result of Pl and Cpx asynchronous crystallization in the reservoirs. MORB data also document the assimilation of at least Ol and/or Pl together with the crystallization of Cpx ± Ol. This result suggests that the extraction of MORB melts from the mush reservoirs proceeds once Cpx has started to crystallize within the mush. It is consistent with the results of Lissenberg *et al.* (2019) who highlighted such a chronology.

The majority of these gabbros, apart from the more evolved lithologies such as oxide gabbros, are described as cumulates based on the whole rock geochemical signatures and especially their incompatible trace element contents which result to some extent from RPF (Fig. 1). Yet, despite several lines of evidence arguing for the occurrence of RPF and some experimental constraints (Leuthold *et al.*, 2015; Yang *et al.*, 2019), the question of the thermodynamic feasibility of RPF process is still pending due to the lack of applied thermodynamic modelling.

Characteristics of the reactions

In detail, the melt-mush reactions described as involved during RPF can vary with the magmatic system considered. On one hand, the reaction characteristics can be estimated relying on the textures and the composition of the studied samples. On the other hand, their impact on the chemistry of a system can be approximated by numerical models. The correspondence between natural chemical compositions and the models then allows adding constraints parameters controlling the reactions, such as the nature and fraction of the reactants and products (melt and minerals). The most commonly used model for RPF relying on trace elements is the assimilation-fractional crystallization model (AFC; DePaolo, 1981). Overall, the reactions mostly involve assimilation and/or crystallization of the main cumulate-

ORIGINAL UNEDITED MANUSCRIPT

Downloaded from https://academic.oup.com/petrology/advance-article/doi/10.1093/petrology/egad005/6998539 by guest on 13 February 2023

forming minerals (i.e., Ol, Pl and Cpx) in various proportions, usually in favor of Ol and Pl assimilation, and crystallization of Pl and Cpx (Fig. 3A, Table 1). This is directly supported by the evidence for Ol and Pl resorbed textures, and evidence for Pl and Cpx crystallization after a first mineral dissolution step (poikilitic minerals engulfing resorbed grains, Fig. 2, Table 1). We present in Fig. 4 different theoretical reactions involving Ol, Pl or Cpx, which are either assimilated or crystallized, both generations of minerals having different compositions. The results show the sensibility of the AFC models to the nature of the phases involved, leading to both enrichment and fractionation between incompatible trace elements that significantly vary with the minerals considered. The composition of the reactive melt is almost systematically more primitive compared to the liquid in equilibrium with the mush crystals involved during the reactions (e.g., (Boulanger et al., 2020)) and, overall, induces reactions in favor of crystallization compared to assimilation, as described by the r ratio in the AFC models from the literature. This r value is described by DePaolo (1981) as the ratio between the rate of assimilation and "the rate at which fractionating phases are being effectively separated from the magma". This ratio is always comprised between 0.5 and ~0.9 in AFC model related to oceanic igneous reservoirs, and usually a range of r is needed to explain the entire range of compositions recorded in a single sample or magmatic system (examples shown in Fig. 3B; literature synthesis present in Table 1; e.g., Coogan *et al.*, 2000; Kvassnes, 2004; Boulanger *et al.*, 2020; Zhang *et al.*, 2020; Ferrando *et al.*, 2021b). The upper limit of r = 0.3 mentioned by DePaolo (1981) for the model applies only to the assimilation of cold country rocks, and r can reach values up to 1 during the assimilation of minerals relatively closer to their liquidus than their solidus temperatures. The range r = 0.2–0.99 summarized in Table 1 therefore likely indicates that melts crystallize and thus tend to reduce the porosity of the system during RPF. It does not ensure, however, that the assimilation and crystallization steps are fully synchronous during melt-mush reaction, even

ORIGINAL UNEDITED MANUSCRIPT

Downloaded from https://academic.oup.com/petrology/advance-article/doi/10.1093/petrology/egad005/6998539 by guest on 13 February 2023

though both are described at the same time by the AFC equation and recorded together in natural samples (Lissenberg and Dick, 2008; Boulanger *et al.*, 2020). The characteristics of the main reactions (type, proportions and compositions of assimilated and crystallized minerals, melt composition) based on the study of natural oceanic crust samples are supported by the results of the few available experimental studies for melt-mush reactions (Leuthold *et al.*, 2015; Yang *et al.*, 2019). They are also consistent with the melt dynamics within magma reservoirs that predict multiple primitive melt injections within crystal mushes and potential large-scale melt percolation (e.g., Grimes *et al.*, 2008; Godard *et al.*, 2009; Sanfilippo and Tribuzio, 2013; Dick *et al.*, 2019; Boulanger *et al.*, 2020; Zhang *et al.*, 2020). Hence, the geochemical signatures of many gabbroic cumulates recovered from the oceanic crust seem to be directly linked to RPF processes, that likely exert a strong control on melt differentiation. We provide in the following a thermodynamic modeling of the potential reactions occurring in gabbroic magma reservoirs to discuss further the implication of melt-mush reactions involved during RPF.

Thermodynamic feasibility test

Aim of the AFC model

We present here an attempt to discuss the thermodynamic feasibility of melt-mush reactions associated with RPF that so far were mostly approached by mass-balance models relying on trace elements and petrographic descriptions (e.g., Sanfilippo *et al.*, 2020; Boulanger *et al.*, 2021; Ferrando *et al.*, 2021b). Our approach complements the work of Collier and Kelemen (2010) that focused on reactive crystallization in the mantle. In our case, the reactions occur in the earliest stages of evolution of a mush in contact with a primitive melt. In this scenario, the mineral assemblage of the mush involved in the reaction(s) formed most likely by FC from a primitive melt (similar to the reactive primitive melt) during a melt-

ORIGINAL UNEDITED MANUSCRIPT

Downloaded from https://academic.oup.com/petrology/advance-article/doi/10.1093/petrology/egad005/6998539 by guest on 13 February 2023

rich evolution phase of the reservoir. The small composition difference and close equilibrium temperatures of the two components (melt and minerals) questions the assimilation capacity of the melt. The thermodynamic model rhyolite-MELTS (Gualda *et al.*, 2012; Ghiorso and Gualda, 2015) allows to model assimilation of a determined mass of material in a melt under isenthalpic conditions. It does not however consider any heat input from the assimilated material on the system. The Magma Chamber Simulator (MCS; Bohrson *et al.*, 2014, 2020), which relies on the rhyolite-MELTS engine, allows to track the enthalpy and both compositions and temperatures of up to three components in a magmatic system : the main magma subsystem, a subsystem assimilated by the magma and a recharge subsystem. Here, we used the AFC mode of the MCS to model the evolution of a mush equivalent when in contact with and assimilated by a primitive melt, with no additional melt input (recharge) during the reaction. The model allows to track the compositional and thermal evolution of both the primitive melt (*Magma*) and of the potentially assimilated material (hereafter called *Mush*) until both are in thermal equilibrium (this is a limit of the MCS AFC model). It also allows to track if any assimilation of the *Mush* was induced.

Model inputs for oceanic crustal reservoirs

We adapted the model to a slow-spreading oceanic environment and used the Atlantis Bank OCC as reference (Boulanger *et al.*, 2020). The *Magma* corresponds to a primitive MORB equivalent suspected to feed the magma reservoirs by cyclic intrusions (SWIR MORB from Coogan *et al.*, 2004 ; described in Boulanger *et al.*, 2020). The *Mush* equivalents (to be assimilated) for the Atlantis Bank system are taken as the mineral assemblages (crystals without melt) obtained by FC of the same primitive MORB equivalent or *Magma* at different temperatures (determined by rhyolite-MELTS). The pressure of the system is set at 2 kbar, with redox conditions at FMQ with ~0.2 wt% H_2O in the *Magma*, which correspond to average estimates for magma reservoirs at slow-spreading ridges (Lissenberg *et al.*, 2015;

ORIGINAL UNEDITED MANUSCRIPT

Downloaded from https://academic.oup.com/petrology/advance-article/doi/10.1093/petrology/egad005/6998539 by guest on 13 February 2023

Koepke *et al.*, 2018). Other parameters for the AFC runs are the enthalpy convergence step optimized by MCS modelers at 30, and the FmZero that we set here at 0.05 as we consider a mineral assemblage from a mush where melt extraction is favored. FmZero describes the proportion of melt to reach in the *Mush* so that partial melts start being extracted from the *Mush* and assimilated in the *Magma*. A decisive input parameter for the system is the temperature set for the different components. The possible input temperatures of the *Mush* using the MCS is either equal or lower than the solidus temperatures of the selected phase assemblages. Two mush compositions were tested, a first early stage cumulate obtained after 17.6% FC by MELTS at 1202°C (18.3% Ol, 61.3% Pl and 20.4% Cpx), and a second advanced stage cumulate obtained at 50.6% FC at 1162°C (11.4% Ol, 52.4% Pl and 36.2% Cpx). The corresponding modal compositions of the considered mushes are consistent with the range of olivine gabbros from Atlantis Bank (Boulanger *et al.*, 2021; Ferrando *et al.*, 2021b). The two corresponding input *Mush* temperatures are taken as their crystallization temperatures of 1202°C for the early stage cumulate and of 1162°C for the advanced stage cumulate. In relation with MCS limitations, the assimilated material had to be fully solidified and we therefore took an adcumulate equivalent to the mush presented above (dry assemblage devoid of melt). This represents an extreme case where the interstitial melt is entirely replaced by the assimilating melt. This extreme case is disadvantageous for assimilation. In a least extreme case, the interstitial melt of a mush could partially to fully mix with the injected primitive melt. The temperature of the melt at the launch of the temperature equilibration between the Magma and the Mush is the liquidus, here at 1256.8°C. We consider a temperature decrement step of 5°C (like the FC model). Finally, and to test the efficiency of the reactions, five ratios of the *Mush*/*Magma* masses of 0.25, 0.5, 1, 1.5 and 2 were considered. They allow to test the reactions for either mush-dominant or melt-dominant regimes and how this parameter influences the temperature equilibrium, and hence the

ORIGINAL UNEDITED MANUSCRIPT

Downloaded from https://academic.oup.com/petrology/advance-article/doi/10.1093/petrology/egad005/6998539 by guest on 13 February 2023

capacity of assimilation of the melt. The inputs and main outputs of the models are presented in the Supplementary Materials Table S3 and in the following section *Results of the melt-mush reaction models*.

The aim of this model is not to reproduce the complete RPF process, but only to test with these endmember reactions if the (small) degree of disequilibrium between the *Magma* and the *Mush* is sufficient to induce assimilation. An integrated RPF model would require a time component and consider the evolution of the permeability within the system during the reactions, which is not possible via the MCS AFC model. The occurrence of assimilation however is often debated and remains a strong argument against melt-mush reactions and RPF process. The inputs presented above were carefully selected to represent the first increment of reaction occurring in the initial phase of the RPF involving a primitive melt and two mineral assemblages that both contain all three main cumulate forming minerals (Ol, Pl and Cpx) suspected to be involved in melt-mush reactions described in natural samples, and on which the models rely.

Results of the melt-mush reaction models

The results of the models are presented in Fig. 5. Fig. 5A details the amount of material from the *Mush* assimilated into the *Magma* and the amount of material crystallized from the *Magma* for each AFC run. The ratio between the total assimilated mass and the total crystallized mass is taken as a proxy to the r ratio discussed earlier in the literature (see **Characteristics of the reaction**). Fig. 5B compares the initial and final state of the *Mush* for each AFC model, in terms of mass of each mineral present. For example, in Fig. 5B no spinel is present in the initial *Mush* and spinel only crystallizes from the *Magma* during the reactions, as shown in Fig. 5A. The equilibrium temperature between the *Mush* and *Magma* reached at the end of the models is between 1219-1242°C for the early stage cumulates and between 1197-1231°C for the advanced stage cumulates. The amount of crystallized and

ORIGINAL UNEDITED MANUSCRIPT

Downloaded from https://academic.oup.com/petrology/advance-article/doi/10.1093/petrology/egad005/6998539 by guest on 13 February 2023

assimilated material is higher for the most evolved *Mush* and increases when the initial amount of *Mush* involved in the reaction is higher (Fig. 5). Overall, the reactions are in favor of assimilation for melt-dominated reactions (*Mush*/*Magma* < 1), with equivalent r ratios between 2.66 and 3.65. For higher *Mush*/*Magma* ratios, no assimilation occurs during the reactions with the early stage (primitive) *Mush*, only crystallization is induced by the decrease in temperature during equilibration with the mush. For the advanced stage (evolved) *Mush*, mush-dominated reactions lead to partial assimilation of the *Mush* but overall, the reactions are in favor of crystallization (with r ratios between 0.65 and 0.90). All three minerals present in the *Mush* are assimilated, mostly Pl, then Cpx, and to lesser extent Ol. This is consistent with Pl and Cpx being in greater disequilibrium with the primitive melt around 1197-1242°C as they form at lower temperature than Ol in this system, and hence are more likely to be assimilated during the temperature equilibration. All minerals crystallize in at least one of the reactions (Spinel, Ol and Pl), except Cpx that is only assimilated in all reactions. Spinel and Ol crystallize in all reactions (the former due to the presence of Cr in the *Magma*), and Pl crystallizes for *Magma*/*Mush* ratios superior or equal to 1. As mentioned earlier, the amount of crystallized and assimilated material increases when the initial amount of *Mush* involved in the reaction is higher (Fig. 5) until no assimilation is possible, which is the case during mush-dominated reactions for the primitive *Mush*. There are two competing mechanisms at play: higher *Mush*/*Magma* ratios imply larger *Mush* mass available for assimilation which seem to favor higher r values (*Mush*/*Magma* up to 1), but at the same time higher initial mass of *Mush* leads to equilibration down to lower temperatures that favor crystallization (*Mush*/*Magma* superior to 1).

Overall, the main results of the new models is that reactions between a mush (primitive or more evolved) and a primitive melt are thermodynamically feasible. For melt-dominated reactions they lead to partial assimilation of the mush crystals with predominant

ORIGINAL UNEDITED MANUSCRIPT

Downloaded from https://academic.oup.com/petrology/advance-article/doi/10.1093/petrology/egad005/6998539 by guest on 13 February 2023

assimilation over crystallization compared to the reactions described in the literature and relying on natural samples (Fig. 3B). Assimilation is also possible during mush-dominated reactions, but it seems to be efficient only for lower-temperature or more evolved assemblages. The associated r values (0.65, 0.72 and 0.9) are more consistent with the range of values described in the literature (Table 1). However, it is difficult to establish with MCS models whether temperature or composition is the controlling parameter. Overall, between ~6 and 21% of the initial *Mush* mass is assimilated during these one-step reactions. The proportion of minerals involved differs from the reactions described in the literature (Table 1). Ol and Pl mainly crystallize in the models whereas in the natural samples Pl and mostly Cpx seem to crystallize during reactions. In addition, Cpx is systematically assimilated during the reactions even though in natural samples ubiquitous textural evidence for such assimilation are so far lacking. These discrepancies could be explained by the fact that our models using the MCS only reproduce one step of melt-mush reactions (until thermal equilibration between *Magma* and *Mush*) in a thermally isolated system, whereas natural samples record the entire protracted RPF process. Also, they do not account for the global progressive cooling of magma reservoirs within the oceanic crust, which eventually lead to complete mush crystallization during which most of Cpx crystallization might occur. These models however support the idea that, as previously suspected (Lissenberg and Dick, 2008; Boulanger *et al.*, 2020), RPF related assimilation and crystallization as recorded in natural samples are partially decoupled. Most of the assimilation likely occurs in the earliest stages of RPF while the melt input is sustained (melt-dominated reactions with $r < 1$). This also means that the permeability of the system can be maintained during the melt-dominated stage of RPF while a new generation of minerals forms at the expanse of the initial mush forming minerals. The one-step AFC models provided here to study crystal-melt interactions are quite decisive as they

ORIGINAL UNEDITED MANUSCRIPT

Downloaded from https://academic.oup.com/petrology/advance-article/doi/10.1093/petrology/egad005/6998539 by guest on 13 February 2023

show for the first time the thermodynamic sustainability of the reactions on which the RPF described relies within oceanic igneous reservoirs.

THE MELT FLUSH PROCESS

Description of the process

We propose here an alternative process for the formation of igneous rock bearing cumulate signatures, which combines the main characteristics of RPF processes with melt dynamics in igneous reservoirs. The *melt flush* process considers the most recent developments on the nature of oceanic reservoirs (mush-dominated), their formation (repetitive cycles of melt intrusions), and associated melt dynamics (melt percolation through the porosity of a mush column). It also relies on the studies of natural samples that show the ubiquitous occurrence of melt-mush reactions and help to precise the main characteristics of these reactions through the textural record and geochemical signatures (see section **Impact of reactive porous flow** above). The process is also strengthened by the new thermodynamic models for melt-mush reactions presented herein, which confirm the thermodynamic feasibility of those reactions.

Overall, the *melt flush* process applies to open system magma reservoirs, in mush-dominated environments continuously fed by primitive melts, subject to global upward melt migration and extraction. Buoyancy associated with the continuous injection of primitive melt in the system appears as the main favorable driving force for melt percolation through a crystal-rich matrix, considering that the bulk density of the cumulate assemblages are denser than the melt (here crystallized from a primary MORB; Lissenberg *et al.*, 2019). Within the considered mush, and because of this internal melt migration, RPF seems to exert a strong control on melt differentiation. As described earlier (EVOLUTION OF OCEANIC IGNEOUS RESERVOIRS), most of the reactions occur between already formed mush crystals and a

ORIGINAL UNEDITED MANUSCRIPT

Downloaded from https://academic.oup.com/petrology/advance-article/doi/10.1093/petrology/egad005/6998539 by guest on 13 February 2023

499 percolating, primitive melt (Fig. 6). The more primitive character of the injected melt relative
500 to the last increment of crystallized minerals implies its thermodynamic disequilibrium with
501 the percolated crystal matrix resulting in interactions (Fig. 6). A simplified view of the *melt*
502 *flush* process could be summarized by the initial crystallization of a relatively primitive melt
503 (L_n) to form a mush composed of crystals (C_{n+1}) that are in equilibrium with a slightly more
504 evolved melt (L_{n+1}) following the reaction ($L_n \rightarrow C_{n+1} + L_{n+1}$). During the first increment of
505 the reactive process, L_n is recharged and percolates through the mush, replacing the interstitial
506 melt (L_{n+1}) that percolates further up in the surrounding mush. At that stage, the interstitial
507 melt (L_{n+1}) is either totally flushed out or partially mixes with the recharge melt (L_n). This
508 triggers a thermodynamic disequilibrium (C_{n+1} is in contact with L_n instead of L_{n+1}) and melt-
509 mush reaction proceeds (Fig. 6). According to our model results, up to 21% of the initial mush
510 crystals (C_{n+1}) is assimilated while a new generation of minerals form (C_{n+2}). These minerals
511 crystallize from the new, more primitive interstitial melt (L_{n+2}) in comparison to the previous
512 interstitial melt (L_{n+1}). L_{n+2} will be similarly flushed out in its turn by a new injection of L_n at
513 the second increment of the reactive process. At the scale of the mush column melt
514 percolation proceeds upwards, and at each level interstitial melts are being progressively
515 flushed up by more primitive melts that evolve through local melt-mush reactions, which
516 defines RPF (Fig. 7A). Crystallization being overall predominant over assimilation in natural
517 cooling reservoirs (Table 1), RPF leads to a progressive record of the primitive character of
518 the recharge melt(s) in the newly formed minerals until the process eventually stops at
519 porosity closure of the system.

520 **Melt flush as a cumulate forming process**

521 The *melt flush* process eventually represents a new endmember to form cumulus rocks.
522 The continuous replacement of the evolved interstitial melt ($_{Ln+1}$) by a more primitive (and
523 thus more depleted in incompatible elements) L_n melt during the *melt flush* process represents

ORIGINAL UNEDITED MANUSCRIPT

Downloaded from https://academic.oup.com/petrology/advance-article/doi/10.1093/petrology/egad005/6998539 by guest on 13 February 2023

524 a key element to acquire a depleted bulk rock composition typical of the cumulate signature.
525 Indeed, incompatible elements that concentrate in the interstitial melt phase during the
526 increment of crystallization are flushed out of the mush and replaced by the more primitive
527 (relatively poorer in incompatible elements) L_n recharge melt. The following crystallization
528 stage being associated with the recharge melt, the depleted cumulate signature is ultimately
529 recorded in the plutonic rock's bulk chemical composition.

530 **Impact on differentiating mush columns and magma reservoirs**

531 The *melt flush* process translates petrographic and geochemical observations from
532 oceanic systems, and together with our new thermodynamic constraints, reconciles the
533 emerging vision of magma reservoirs and their formation dynamics with the widespread
534 record of RPF in plutonic (and volcanic) rocks. The process is also consistent in terms of melt
535 dynamics with the complex replenish-mix-tap-crystallize model (RMTX, O'Neill and Jenner,
536 2016) that would, in the *melt flush* case, integrate an additional assimilation component. In
537 fact, even in the RMTX model, assimilation is likely to proceed as this model considers a
538 recharge stage within a partially crystallized system. No direct physical constraints are
539 established at this stage, apart from the density characterization of the solid and liquid phases
540 of the magmatic systems driving melt buoyancy and migration through the mush. The
541 question of the feasibility and stability of the flow involved during RPF can be a matter of
542 debate, which we do not aim to fully address here, but recent numerical simulations in
543 continental settings seem to highlight the viability of this process at the crustal scale. Again
544 there, the process is triggered by continuous melt recharge and buoyancy (Jackson *et al.*,
545 2018). The results of the melt-mush reaction models presented here are also consistent with
546 the *melt flush*: if the porous flow is sustained through the mush, preventing cooling of the
547 magma reservoir at the large scale, the melt-mush reactions leading to both assimilation and
548 crystallization should locally stay in favor of assimilation, hence preventing total porosity

ORIGINAL UNEDITED MANUSCRIPT

Downloaded from https://academic.oup.com/petrology/advance-article/doi/10.1093/petrology/egad005/6998539 by guest on 13 February 2023

closure and maintaining permeability in the system. The physical conditions associated with melt migration likely vary with and within the system considered, which would also partially explain the variability in textures and geochemical signatures recorded within gabbro cumulates (e.g., Ferrando *et al.*, 2021b). The efficiency of melt replacement and extraction associated with *melt flush* is also important to consider, especially in the presence of melts (interstitial and replacing) with high viscosity contrasts. High viscosity differences generate instabilities (Saffman-Taylor, e.g., Whitehead and Helfrich, 1991; Perugini and Poli, 2005) that lead to viscous fingering structures and "focused" flow of low viscosity melts in high viscosity ones. Considering the *melt flush* process, the iterative melt migration from one level to the next one in a mush column likely proceeds on relatively short distances (meter scale, see Ferrando et al., 2021b, who highlighted the presence of reactive melt extraction every 3 to 4 m in the studied plutonic section), and viscosity variations are therefore very limited on a local scale. In this perspective, Saffman-Taylor instabilities are unlikely to occur, even less so if mixing occurs between melts. As an example, for tholeiitic systems, after 60% crystallization the viscosity of the differentiating melt only increases by a factor of 1.3 (MELTS FC of the primitive MORB composition from the SWIR (Gualda *et al.*, 2012). Protracted differentiation of melts is not excluded by *melt flush* but would occur at the scale of the entire mush column with differentiation and viscosity increasing gradually towards the top of the system and melt density progressively decreasing and sustaining buoyancy flow.

GENERALIZATION AND LIMITS OF THE PROCESS

The *melt flush* process potentially applies to any magmatic system that shares the same characteristics considered here for oceanic magma reservoirs and presented in the following. As described earlier (**INTRODUCTION**), 1/ the incremental formation of magma chambers or reservoirs thanks to multiple melt injections is almost consensual (e.g., Annen *et al.*, 2015;

ORIGINAL UNEDITED MANUSCRIPT

Downloaded from https://academic.oup.com/petrology/advance-article/doi/10.1093/petrology/egad005/6998539 by guest on 13 February 2023

Hepworth *et al.*, 2018; Sparks *et al.*, 2019). The other fundamental characteristic of magma reservoirs where *melt flush* is potentially occurring is 2/ the presence of mush. The mush-dominated character of the reservoirs is sometimes debated in other settings than at oceanic spreading centers, and evidence for melt evolution in mostly liquid chamber or sills were presented and long suspected in different systems (e.g., most recently in the Bushveld Complex, Holness *et al.*, 2017a; Kruger and Latypov, 2020; and elsewhere, Holness *et al.*, 2019). However, many models suggest that at least part or most of melt storage and/or evolution at depth occurs on long timescales in a mushy medium (e.g., Bachmann and Bergantz, 2008; Cashman *et al.*, 2017; Cooper, 2017; Jackson *et al.*, 2018; Edmonds *et al.*, 2019, and references therein). This is especially the case for transcrustal mgmatic systems where the presence of mush is supported by geophysical evidence (Huang *et al.*, 2015; Kiser *et al.*, 2016), and in which 3/ reactive melt flow is expected to be a critical process for melt differentiation (Cashman *et al.*, 2017; Jackson *et al.*, 2018; Blundy, 2022). The process would lead to a decoupling between major and trace elements (Solano *et al.*, 2014; Blundy, 2022), which is similar to the evolution of the geochemical signatures described as characteristic of RPF in oceanic systems. A growing number of evidence for the occurrence of melt-mush reactions is described in various magmatic systems apart from mid-ocean ridges. In the Rum Layered Intrusion (Scotland), the layered structure represents crosscutting sills formed by repeated intrusion of picritic melts (Holness *et al.*, 2007; Hepworth *et al.*, 2018; Troll *et al.*, 2020). Several lines of evidence for melt-mush reactions (or infiltration metasomatism) were found in Units 7 to 12 linked to these intrusive events within pre-existing cumulates, with wavy reaction fronts associated with upward reactive melt infiltration or laterally orientated metasomatism (Holness *et al.*, 2007; O'Driscoll *et al.*, 2010; Leuthold *et al.*, 2014, 2015; Hepworth *et al.*, 2020). At Skaergaard Intrusion (East Greenland), evidence for RPF has not been identified directly within the layered sequence but within the Marginal Border Series,

ORIGINAL UNEDITED MANUSCRIPT

Downloaded from https://academic.oup.com/petrology/advance-article/doi/10.1093/petrology/egad005/6998539 by guest on 13 February 2023

599 which represent the mushy inner margin of the intrusion where infiltration of reactive melts
600 and progressive margin growth occurred (Namur *et al.*, 2013). Geochemical maps of P in Ol
601 from the Sept Iles layered intrusion show evidence of complex zoning with intense dissolution
602 features highlighting intense interactions between the crystals and a disequilibrium melt (Xing
603 et al., 2022). Evidence for melt-mush reactions was also found in the arc crust. Within the
604 lower arc crust exposed at the Sapat Complex (Pakistan), Bouilhol *et al.* (2015) identified
605 feeder pipes of mantle melts concomitantly evolving and reacting with previous cumulates
606 while arising through the km-scale structures. On another scale, plutonic xenoliths from
607 Martinique sampling mid-crust crystal mushes reveal the occurrence of melt-mush reactions
608 within the system, yet this information appears to be lacking within lavas (Cooper *et al.*,
609 2016). Finally, ocean island systems are not exempt from RPF, as Gleeson *et al.* (2021)
610 detected evidence for melt-mush reactions in both xenoliths and erupted magmas from the
611 low melt input mushy magma reservoir beneath Isla Floreana (Galapagos, Ecuador). The
612 characteristics of the reactions detailed in those various studies are summarized in Table 1.
613 Compared to mid-ocean ridges, the reactions associated with RPF are nevertheless not yet
614 characterized to the same extent or resolution in other crustal magmatic systems. The impact
615 of RPF on melt differentiation is key to assess the potential implications of the *melt flush*
616 process in those systems and is still challenged. Hence, a better comprehension of the
617 potential implication of RPF is required before any attempt to generalize the *melt flush*
618 process to other magmatic systems, even though the other main characteristics of the
619 magmatic systems involved are met.

620 The *melt flush* process also has potential implications on the collection, aggregation
621 and accumulation of melt-rich bodies at or close to the top of mush columns. At fast-
622 spreading oceanic ridges, or in some continental series like in the Ivrea-Verbano zone, where
623 plumbing systems have been interpreted to be transcrustal, the cumulative series are topped

ORIGINAL UNEDITED MANUSCRIPT

Downloaded from https://academic.oup.com/petrology/advance-article/doi/10.1093/petrology/egad005/6998539 by guest on 13 February 2023

by relatively evolved plutonics when compared to the underlying more mafic series (e.g., Voshage *et al.*, 1990; MacLeod and Yaouancq, 2000; France *et al.*, 2009). Similar features are observed at the top of mushy igneous reservoirs from slow-spreading oceanic centers (Boulanger *et al.*, 2020) on which the *melt flush* process relies. Although detailed models dedicated to each of those settings would be required to fully apprehend the corresponding processes, this common feature could potentially be explained by the numerical models presented by Jackson *et al.* (2018) who highlighted that incrementally formed transcrustal igneous systems tend to develop more evolved melt-rich bodies in their relatively shallow levels through reactive melt flow. In continental settings, where transcrustal plumbing systems are likely thicker than in oceanic settings, differentiation is potentially more pronounced, and the *melt flush* process, if effective, could be protracted with the intrusion of significantly higher volumes of primitive melt at the bottom of the system, and over longer periods of time. The production of larger volumes of potentially more evolved melts in the upper part of the mush column could be amplified, and the assimilation component of RPF could also assist crystal repacking that is the most likely process inducing silicic melt extraction from a crystal matrix (Bachmann and Huber, 2019). The *melt flush* process and associated evolved melt extraction close to shallow levels, thus potentially relates to the process of formation of large volumes of silica-rich melts feeding large silicic eruptions.

PERSPECTIVES

The *melt flush* process does not aim to replace other cumulate forming processes, and where occurring, it likely acts concomitantly to crystal settling, mush compaction or deformation, and reinforces the geochemical cumulate signatures recorded in plutonic rocks (Fig. 7B). The scale in both time and space at which the *melt flush* process applies is also likely to vary depending on the magmatic system considered (size of the reservoir, melt input

ORIGINAL UNEDITED MANUSCRIPT

Downloaded from https://academic.oup.com/petrology/advance-article/doi/10.1093/petrology/egad005/6998539 by guest on 13 February 2023

649 volumes and fluxes, duration of the magmatic activity, localization of the mush zones). The
650 process as presented here relies on our current knowledge of RPF, and mostly considers
651 petrographic, geochemical and new thermodynamic constraints, yet the latter only regards the
652 feasibility of end-member melt-mush reactions in a static way. The modelling of RPF itself,
653 that is necessary to test the implications of *melt flush* for magmatic systems, requires the
654 consideration of physical parameters to constrain the evolution of the system during the
655 reactions: the evolution of the porosity, its impact on the permeability of the system, the
656 viscosity and relative buoyancy of the melt(s) compared to the mineral assemblages, and the
657 deformability of the mush matrix. Indeed, these parameters control the capacity of the melt(s)
658 to percolate through the mush, and hence the occurrence and efficiency of RPF. Time, and
659 melt flux constraints will also have to be implemented if we are to better apprehend the
660 kinematics of the *melt flush* process, the degree of reequilibration between newly injected
661 melt(s) and the percolation matrix, and thus the final mineral (and melt) compositions.

662 Although additional physical constraints will be required to better apprehend the *melt*
663 *flush* process, it represents a novel, first-order igneous process integrating for the first time (1)
664 the emerging vision of magmatic reservoirs as mush-dominated environments, (2) their
665 formation dynamics as open magmatic systems subject to repeated melt intrusions, and (3) the
666 widespread record of RPF in both plutonic and volcanic rocks and the chemical contribution
667 of migrating melts during cumulate formation.

668

669 **CONCLUSION**

670 The current concept of magma reservoirs has been shifting over the past decades from
671 liquid- to mush-dominated environments. The implication of mush as the predominant
672 differentiation medium of crustal melts is potentially significant but not yet integrated at the
673 scale of magma reservoirs or crustal accretion. In slow-spreading mid-oceanic ridge

ORIGINAL UNEDITED MANUSCRIPT

Downloaded from https://academic.oup.com/petrology/advance-article/doi/10.1093/petrology/egad005/6998539 by guest on 13 February 2023

reservoirs, the occurrence and significance of crystal-melt interactions within mushes have been described in multiple samples, magmatic systems, and at multiple scales. The summary of the RPF models shows similarities between the reactions, which often involve a primitive melt interacting with the main mush minerals (Ol, Pl, Cpx) under a prevailing crystallization regime over assimilation. Modeling of those melt-mush reactions using here the Magma Chamber Simulator shows their thermodynamic feasibility and supports their widespread occurrence in nature. The RPF characteristics that are determined by the petrology and compositions of natural samples are also consistent with the global melt dynamics within oceanic magma systems, formed by cyclic melt intrusions at depths during the main magmatic events. Altogether, this opens the potential for revisiting some concepts for the formation of igneous reservoirs, and especially here for the formation of igneous cumulates. Classical formation processes (melt buoyancy, crystal-mush compaction) are either insufficient on their own or not observed in many oceanic igneous cumulates, and we attempt here to propose a novel igneous process that accounts for the widespread occurrence of RPF, and for melt dynamics within reservoirs: the *melt flush* process. During the *melt flush*, the cyclic inputs of primitive melts at the base of a mush column together with buoyancy (of melts relative to crystals) prompt the flushing out of the interstitial, more evolved melt out of the system. Primitive melts interact with the mush crystals in disequilibrium, which are partially assimilated during melt-mush reactions while a new generation of minerals forms from the reactive melt. These minerals record a cumulative geochemical signature through the replacement of interstitial evolved melt by the reinjected more primitive one, together with the record of the associated RPF signatures. The *melt flush* process does not aim at replacing other processes for the formation of cumulates that likely acts jointly to some degree, but is a reconciliation with our current understanding of oceanic igneous reservoirs by taking into account primitive melt inputs in the systems, and the widespread occurrence of RPF. The *melt*

ORIGINAL UNEDITED MANUSCRIPT

Downloaded from https://academic.oup.com/petrology/advance-article/doi/10.1093/petrology/egad005/6998539 by guest on 13 February 2023

flush opens the way for new discussion for example on the physics of the reservoirs and mushes, in addition to the completion of integrated thermodynamic models at the scale of magma reservoirs. The process is potentially applicable to some degree to magmatic systems sharing the same characteristics as slow-spreading mid-ocean ridge reservoirs, i.e. the presence of mush, cyclic melt recharges, and the widespread occurrence of RPF.

SUPPLEMENTARY DATA

Supplementary data are available at Journal of Petrology online.

ACKNOWLEDGMENTS

We thank Olivier Bachmann, Céline Baudouin, Pierre Bouilhol, Mathilde Cannat, Katharine V. Cashman, Jeremy R.L. Deans, Carlotta Ferrando and Marguerite Godard for helpful discussions. LF thanks Henry Dick, Chris MacLeod and Jim Natland for passionate discussions about cumulate formation. This contribution also considerably benefited from Journal of Petrology reviewers and perspective editor Jörg Hermann. This project has been supported by IODP-France and INSU-CNRS. This is CRPG contribution n°xxxx.

ORIGINAL UNEDITED MANUSCRIPT

Downloaded from https://academic.oup.com/petrology/advance-article/doi/10.1093/petrology/egad005/6998539 by guest on 13 February 2023

716 **References**

717 Annen, C., Blundy, J. D., Leuthold, J. & Sparks, R. S. J. (2015). Construction and evolution
718 of igneous bodies: Towards an integrated perspective of crustal magmatism. *Lithos*.
719 Elsevier B.V. **230**, 206–221.

720 Annen, C., Scaillet, B. & Sparks, R. S. J. (2006). Thermal constraints on the emplacement rate
721 of a large intrusive complex: The Manaslu Leucogranite, Nepal Himalaya. *Journal of*
722 *Petrology* **47**, 71–95.

723 Bachmann, O. & Bergantz, G. W. (2003). Rejuvenation of the Fish Canyon magma body: A
724 window into the evolution of large-volume silicic magma systems. *Geology* **31**, 789–
725 792.

726 Bachmann, O. & Bergantz, G. W. (2004). On the origin of crystal-poor rhyolites: Extracted
727 from batholithic crystal mushes. *Journal of Petrology* **45**, 1565–1582.

728 Bachmann, O. & Bergantz, G. W. (2008). Rhyolites and their Source Mushes across ectonic
729 Settings. **49**, 2277–2285.

730 Bachmann, O. & Huber, C. (2019). The Inner Workings of Crustal Distillation Columns; The
731 Physical Mechanisms and Rates Controlling Phase Separation in Silicic Magma
732 Reservoirs. *Journal of Petrology* **60**, 3–18.

733 Bachmann, O., Miller, C. F. & de Silva, S. L. (2007). The volcanic-plutonic connection as a
734 stage for understanding crustal magmatism. *Journal of Volcanology and Geothermal*
735 *Research* **167**, 1–23.

736 Bédard, J. H. (1994). A procedure for calculating the equilibrium distribution of trace
737 elements among the minerals of cumulate rocks , and the concentration of trace elements
738 in the coexisting liquids. *Chemical Geology* **118**, 143–153.

739 Bloomer, S. H., Meyer, P. S., Dick, H. J. B., Ozawa, K. & Natland, J. H. (1991). Textural and
740 mineralogic variations in gabbroic rocks from Hole 735B. *Proceedings of the Ocean*

ORIGINAL UNEDITED MANUSCRIPT

Downloaded from https://academic.oup.com/petrology/advance-article/doi/10.1093/petrology/egad005/6998539 by guest on 13 February 2023

Drilling Program.

Blundy, J. (2022). Chemical Differentiation by Mineralogical Buffering in Crustal Hot Zones. *Journal of Petrology* **63**, 1–36.

Bohrson, W. A., Spera, F. J., Ghiorso, M. S., Brown, G. A., Creamer, J. B. & Mayfield, A. (2014). Thermodynamic model for energy-constrained open-system evolution of crustal magma bodies undergoing simultaneous recharge, assimilation and crystallization: The magma chamber simulator. *Journal of Petrology* **55**, 1685–1717.

Bohrson, W. A., Spera, F. J., Heinonen, J. S., Brown, G. A. & Scruggs, M. A. (2020). Diagnosing open - system magmatic processes using the Magma Chamber Simulator (MCS): part I — major elements and phase equilibria. *Contributions to Mineralogy and Petrology*. Springer Berlin Heidelberg.

Borghini, G. & Rampone, E. (2007). Postcumulus processes in oceanic-type olivine-rich cumulates: The role of trapped melt crystallization versus melt/rock interaction. *Contributions to Mineralogy and Petrology* **154**, 619–633.

Boudreau, A. (2016). Bubble migration in a compacting crystal-liquid mush. *Contributions to Mineralogy and Petrology*. Springer Berlin Heidelberg **171**, 1–17.

Bouilhol, P., Schmidt, M. W. & Burg, J.-P. (2015). Magma Transfer and Evolution in Channels within the Arc Crust: the Pyroxenitic Feeder Pipes of Sapat (Kohistan, Pakistan). *Journal of Petrology* **56**, 1309–1342.

Boulanger, M. (2020). Le devenir des liquides au sein de la croûte océanique des dorsales à expansion lente. *Université de Lorraine*.

Boulanger, M. *et al.* (2021). Magma-Mush Interactions in the Lower Oceanic Crust: Insights From Atlantis Bank Layered Series (Southwest Indian Ridge). *Journal of Geophysical Research: Solid Earth* **126**.

Boulanger, M., France, L., Deans, J. R. L., Ferrando, C., Lissenberg, C. J. & von der Handt,

ORIGINAL UNEDITED MANUSCRIPT

Downloaded from https://academic.oup.com/petrology/advance-article/doi/10.1093/petrology/egad005/6998539 by guest on 13 February 2023

766 A. (2020). Magma Reservoir Formation and Evolution at a Slow-Spreading Center
767 (Atlantis Bank, Southwest Indian Ridge). *Frontiers in Earth Science* **8**.
768 Bowen, N. L. (1915). The later stages of the evolution of the igneous rocks. *journal of*
769 *geology* **XXIII**.
770 Bowen, N. L. (1920). Differentiation by deformation. *Proceedings of the national academy of*
771 *sciences* **6**, 59–62.
772 Bowen, N. L. (1928). *The evolution of the igneous rocks*. .
773 Burgisser, A. & Bergantz, G. W. (2011). A rapid mechanism to remobilize and homogenize
774 highly crystalline magma bodies. *Nature*. Nature Publishing Group **471**, 212–217.
775 Canales, J. P., Dunn, R. A., Arai, R. & Sohn, R. A. (2017). Seismic imaging of magma sills
776 beneath an ultramafic-hosted hydrothermal system. *Geology* **45**, 451–454.
777 Canales, J. P., Nedimovi, M. R., Kent, G. M., Carbotte, S. M. & Detrick, R. S. (2009).
778 Seismic reflection images of a near-axis melt sill within the lower crust at the juan de
779 fuca ridge. *Nature* **460**, 89–93.
780 Cashman, K. V., Sparks, R. S. J. & Blundy, J. D. (2017). Vertically extensive and unstable
781 magmatic systems: A unified view of igneous processes. *Science* **355**.
782 Cheadle, M. J., Elliott, M. T. & McKenzie, D. (2004). Percolation threshold and permeability
783 of crystallizing igneous rocks: The importance of textural equilibrium. *Geology* **32**, 757–
784 760.
785 Cheadle, M. J. & Gee, J. S. (2017). Quantitative textural insights into the formation of gabbro
786 in mafic Intrusions. *Elements* **13**, 409–414.
787 Chen, J., Cannat, M., Tao, C., Sauter, D. & Munschy, M. (2021). 780 Thousand Years of
788 Upper-Crustal Construction at a Melt-Rich Segment of the Ultraslow Spreading
789 Southwest Indian Ridge 50°28′E. *Journal of Geophysical Research: Solid Earth* **126**.
790 Collier, M. L. & Kelemen, P. B. (2010). The case for reactive crystallization at mid-ocean

ORIGINAL UNEDITED MANUSCRIPT

Downloaded from https://academic.oup.com/petrology/advance-article/doi/10.1093/petrology/egad005/6998539 by guest on 13 February 2023

ridges. *Journal of Petrology* **51**, 1913–1940.

Comeau, M. J., Unsworth, M. J., Ticona, F. & Sunagua, M. (2015). Magnetotelluric images of magma distribution beneath Volcán Uturuncu, Bolivia: Implications for magma dynamics. *Geology* **43**, 243–246.

Coogan, L. A. (2014). *The Lower Oceanic Crust. Treatise on Geochemistry: Second Edition*. Elsevier Ltd.

Coogan, L. A., Saunders, A. D., Kempton, P. D. & Norry, M. J. (2000). Evidence from oceanic gabbros for porous melt migration within a crystal mush beneath the Mid-Atlantic Ridge. *Geochemistry, Geophysics, Geosystems* **1**.

Coogan, L. A., Thompson, G. M., MacLeod, C. J., Dick, H. J. B., Edwards, S. J., Hosford Scheirer, A. & Barry, T. L. (2004). A combined basalt and peridotite perspective on 14 million years of melt generation at the Atlantis Bank segment of the Southwest Indian Ridge: Evidence for temporal changes in mantle dynamics? *Chemical Geology* **207**, 13–30.

Cooper, G. F., Davidson, J. P. & Blundy, J. D. (2016). Plutonic xenoliths from Martinique, Lesser Antilles: evidence for open system processes and reactive melt flow in island arc crust. *Contributions to Mineralogy and Petrology*. Springer Berlin Heidelberg **171**.

Cooper, K. M. (2017). What does a magma reservoir look like? the "crystal's-eye" view. *Elements* **13**, 23–28.

Cordier, C., Benoit, M., Hémond, C., Dyment, J., Gall, B. Le, Briais, A. & Kitazawa, M. (2010). Time scales of melt extraction revealed by distribution of lava composition across a ridge axis. *Geochemistry, Geophysics, Geosystems* **11**.

Costa, A., Caricchi, L. & Bagdassarov, N. (2009). A model for the rheology of particle-bearing suspensions and partially molten rocks. *Geochemistry, Geophysics, Geosystems* **10**, n/a-n/a.

ORIGINAL UNEDITED MANUSCRIPT

Downloaded from https://academic.oup.com/petrology/advance-article/doi/10.1093/petrology/egad005/6998539 by guest on 13 February 2023

Daines, M. J. & Pec, M. (2015). Migration of Melt. *The Encyclopedia of Volcanoes* 49–64.

DePaolo, D. J. (1981). Trace element and isotopic effects of combined wallrock assimilation and fractional crystallization. *Earth and Planetary Science Letters* **53**, 189–202.

Desissa, M., Johnson, N. E., Whaler, K. A., Hautot, S., Fisseha, S. & Dawes, G. J. K. (2013). A mantle magma reservoir beneath an incipient mid-ocean ridge in Afar, Ethiopia. *Nature Geoscience*. Nature Publishing Group **6**, 861–865.

Dick, H. J. B. *et al.* (2000). A long in situ section of the lower ocean crust: results of ODP Leg 176 drilling at the Southwest Indian Ridge. *Earth and Planetary Science Letters* **179**, 31–51.

Dick, H. J. B. *et al.* (2019). Dynamic Accretion Beneath a Slow-Spreading Ridge Segment: IODP Hole 1473A and the Atlantis Bank Oceanic Core Complex. *Journal of Geophysical Research: Solid Earth* **124**, 12631–12659.

Dunn, R. A. (2015). Crust and Lithospheric Structure - Seismic Structure of Mid-Ocean Ridges. *Treatise on Geophysics*. Elsevier, 419–451.

Dunn, R. A., Lekić, V., Detrick, R. S. & Toomey, D. R. (2005). Three-dimensional seismic structure of the Mid-Atlantic Ridge (35°N): Evidence for focused melt supply and lower crustal dike injection. *Journal of Geophysical Research B: Solid Earth* **110**, 1–17.

Edmonds, M., Cashman, K. V., Holness, M. & Jackson, M. (2019). Architecture and dynamics of magma reservoirs. *Philosophical Transactions of the Royal Society A: Mathematical, Physical and Engineering Sciences* **377**.

Ferrando, C., Basch, V., Ildefonse, B., Deans, J. R., Sanfilippo, A., Barou, F. & France, L. (2021a). Compaction-driven melt extraction and accumulation in a slow-spreading oceanic crust: microstructures of olivine gabbros from Atlantis Bank (IODP Hole U1473A, SWIR). *Tectonophysics* **815**.

Ferrando, C., France, L., Basch, V., Sanfilippo, A., Tribuzio, R. & Boulanger, M. (2021b).

ORIGINAL UNEDITED MANUSCRIPT

Downloaded from https://academic.oup.com/petrology/advance-article/doi/10.1093/petrology/egad005/6998539 by guest on 13 February 2023

Grain size variations record segregation of melts residual from reactive migration in slow-spreading oceanic crust (Atlantis Bank ; 57°E Southwest Indian Ridge). *J. Geophys. Res.-Solid Earth*.

Ferrando, C., Godard, M., Ildefonse, B. & Rampone, E. (2018). Melt transport and mantle assimilation at Atlantis Massif (IODP Site U1309): Constraints from geochemical modeling. *Lithos*. Elsevier B.V. **323**, 24–43.

France, L., Ildefonse, B. & Koepke, J. (2009). Interactions between magma and hydrothermal system in Oman ophiolite and in IODP Hole 1256D: Fossilization of a dynamic melt lens at fast spreading ridges. *Geochemistry, Geophysics, Geosystems* **10**, 1–30.

Gale, A., Dalton, C. A., Langmuir, C. H., Su, Y. & Schilling, J. G. (2013). The mean composition of ocean ridge basalts. *Geochemistry, Geophysics, Geosystems* **14**, 489–518.

Gao, Y., Hoefs, J., Hellebrand, E., von der Handt, A. & Snow, J. E. (2007). Trace element zoning in pyroxenes from ODP Hole 735B gabbros: Diffusive exchange or synkinematic crystal fractionation? *Contributions to Mineralogy and Petrology* **153**, 429–442.

Ghiorso, M. S. & Gualda, G. A. R. (2015). An H2O–CO2 mixed fluid saturation model compatible with rhyolite-MELTS. *Contributions to Mineralogy and Petrology*. Springer Berlin Heidelberg **169**, 53.

Gleeson, M. L. M., Gibson, S. A. & Stock, M. J. (2021). Upper Mantle Mush Zones beneath Low Melt Flux Ocean Island Volcanoes : Insights from Isla Floreana, Galapagos. *Journal of Petrology* 1–26.

Godard, M. *et al.* (2009). Geochemistry of a long in-situ section of intrusive slow-spread oceanic lithosphere: Results from IODP Site U1309 (Atlantis Massif, 30°N Mid-Atlantic-Ridge). *Earth and Planetary Science Letters*. Elsevier B.V. **279**, 110–122.

Grimes, C. B., John, B. E., Cheadle, M. J. & Wooden, J. L. (2008). Protracted construction of gabbroic crust at a slow spreading ridge: Constraints from 206Pb/238U zircon ages from

ORIGINAL UNEDITED MANUSCRIPT

Downloaded from https://academic.oup.com/petrology/advance-article/doi/10.1093/petrology/egad005/6998539 by guest on 13 February 2023

Atlantis Massif and IODP Hole U1309D (30°N, MAR). *Geochemistry, Geophysics, Geosystems* **9**.

Gualda, G. A. R., Ghiorso, M. S., Lemons, R. V. & Carley, T. L. (2012). Rhyolite-MELTS: A modified calibration of MELTS optimized for silica-rich, fluid-bearing magmatic systems. *Journal of Petrology* **53**, 875–890.

Harris, P. G. (1957). Zone refining and the origin of potassic basalts. *Geochimica et Cosmochimica Acta*, ***12***(3), 195–208. https://doi.org/10.1016/0016-7037(57)90032-7

Hepworth, L. N., Kaufmann, F. E. D., Hecht, L., Gertisser, R. & O'Driscoll, B. (2020). Braided peridotite sills and metasomatism in the Rum Layered Suite, Scotland. *Contributions to Mineralogy and Petrology*. Springer Berlin Heidelberg **175**, 1–25.

Hepworth, L. N., O'Driscoll, B., Gertisser, R., Daly, J. S. & Emeleus, C. H. (2018). Linking in situ crystallization and magma replenishment via sill intrusion in the Rum Western Layered Intrusion, NW Scotland. *Journal of Petrology* **59**, 1605–1642.

Hildreth, W., & Moorbath, S. (1988). Crustal contributions to arc magmatism in the Andes of Central Chile. *Contributions to Mineralogy and Petrology*, **98**(4), 455–489. https://doi.org/10.1007/BF00372365

Holness, M. B. (2018). Melt segregation from silicic crystal mushes : a critical appraisal of possible mechanisms and their microstructural record. *Contributions to Mineralogy and Petrology*. Springer Berlin Heidelberg **173**, 1–17.

Holness, M. B., Cawthorn, R. G. & Roberts, J. (2017a). The thickness of the crystal mush on the floor of the Bushveld magma chamber. *Contributions to Mineralogy and Petrology*. Springer Berlin Heidelberg **172**, 1–20.

Holness, M. B., Hallworth, M. A., Woods, A. & Sides, R. E. (2007). Infiltration metasomatism of cumulates by intrusive magma replenishment: The wavy horizon, Isle of Rum, Scotland. *Journal of Petrology* **48**, 563–587.

ORIGINAL UNEDITED MANUSCRIPT

Downloaded from https://academic.oup.com/petrology/advance-article/doi/10.1093/petrology/egad005/6998539 by guest on 13 February 2023

Holness, M. B., Stock, M. J. & Geist, D. (2019). Magma chambers versus mush zones: Constraining the architecture of sub-volcanic plumbing systems from microstructural analysis of crystalline enclaves. *Philosophical Transactions of the Royal Society A: Mathematical, Physical and Engineering Sciences* **377**.

Holness, M. B., Vukmanovic, Z. & Mariani, E. (2017b). Assessing the role of compaction in the formation of adcumulates: A microstructural perspective. *Journal of Petrology* **58**, 643–674.

Huang, H.-H., Lin, F.-C., Schmandt, B., Farrell, J., Smith, R. B. & Tsai, V. C. (2015). The Yellowstone magmatic system from the mantle plume to the upper crust. *Science* **348**, 773–776.

Irvine, T. N. (1982). Terminology for Layered Intrusions. *Journal of Petrology* **23**, 127–162.

Jackson, M. D., Blundy, J. & Sparks, R. S. J. (2018). Chemical differentiation, cold storage and remobilization of magma in the Earth's crust. *Nature*. Springer US **564**, 405–409.

Kiser, E., Palomeras, I., Levander, A., Zelt, C., Harder, S., Schmandt, B., Hansen, S., Creager, K. & Ulberg, C. (2016). Magma reservoirs from the upper crust to the Moho inferred from high-resolution Vp and Vs models beneath Mount St. Helens, Washington State, USA. *Geology* **44**, 411–414.

Koepke, J., Botcharnikov, R. E. & Natland, J. H. (2018). Crystallization of late-stage MORB under varying water activities and redox conditions: Implications for the formation of highly evolved lavas and oxide gabbro in the ocean crust. *Lithos*. Elsevier B.V. **323**, 58–77.

Kohlstedt, D. L. & Holtzman, B. K. (2009). Shearing melt out of the earth: An experimentalist's perspective on the influence of deformation on melt extraction. *Annual Review of Earth and Planetary Sciences* **37**, 561–593.

Krättli, G. & Schmidt, M. W. (2021). Experimental settling, floatation and compaction of

ORIGINAL UNEDITED MANUSCRIPT

Downloaded from https://academic.oup.com/petrology/advance-article/doi/10.1093/petrology/egad005/6998539 by guest on 13 February 2023

plagioclase in basaltic melt and a revision of melt density. *Contributions to Mineralogy and Petrology*. Springer Berlin Heidelberg **176**, 1–27.

Kruger, W. & Latypov, R. (2020). Fossilized solidifications fronts in the Bushveld Complex argues for liquid-dominated magmatic systems. *Nature Communications*. Springer US **11**, 1–11.

Kvassnes, A. J. S. (2004). The evolution of oceanic gabbros : in situ and ancient examples. MIT - Woods Hole Joint Progra in Oceanography, Woods Hole.

Lambart, S., Koornneef, J. M., Millet, M. A., Davies, G. R., Cook, M. & Lissenberg, C. J. (2019). Highly heterogeneous depleted mantle recorded in the lower oceanic crust. *Nature Geoscience*. Springer US **12**, 482–486.

Langmuir, C. H. (1989). Geochemical consequences of in situ crystallization. *Nature* **340**, 199–205.

Latypov, R. M., Chistyakova, S. Y., Namur, O. & Barnes, S. (2020). Dynamics of evolving magma chambers : textural and chemical evolution of cumulates at the arrival of new liquidus phases. *Earth-Science Reviews*. Elsevier **210**, 103388.

Laumonier, M., Karakas, O., Bachmann, O., Gaillard, F., Lukács, R., Seghedi, I., Menand, T. & Harangi, S. (2019). Evidence for a persistent magma reservoir with large melt content beneath an apparently extinct volcano. *Earth and Planetary Science Letters*. Elsevier B.V. **521**, 79–90.

Lejeune, A. M. & Richet, P. (1995). Rheology of crystal-bearing silicate melts: an experimental study at high viscosities. *Journal of Geophysical Research* **100**, 4215–4229.

Leuthold, J., Blundy, J. D. & Brooker, R. A. (2015). Experimental petrology constraints on the recycling of mafic cumulate: a focus on Cr-spinel from the Rum Eastern Layered Intrusion, Scotland. *Contributions to Mineralogy and Petrology*. Springer Berlin

ORIGINAL UNEDITED MANUSCRIPT

Downloaded from https://academic.oup.com/petrology/advance-article/doi/10.1093/petrology/egad005/6998539 by guest on 13 February 2023

Heidelberg **170**, 12.

Leuthold, J., Blundy, J. D., Holness, M. B. & Sides, R. (2014). Successive episodes of reactive liquid flow through a layered intrusion (Unit 9, Rum Eastern Layered Intrusion, Scotland). *Contributions to Mineralogy and Petrology* **168**, 1–27.

Leuthold, J., Lissenberg, C. J., O'Driscoll, B., Karakas, O., Falloon, T., Klimentyeva, D. N. & Ulmer, P. (2018). Partial Melting of Lower Oceanic Crust Gabbro: Constraints From Poikilitic Clinopyroxene Primocrysts. *Frontiers in Earth Science* **6**.

Lissenberg, C. J. & Dick, H. J. B. (2008). Melt-rock reaction in the lower oceanic crust and its implications for the genesis of mid-ocean ridge basalt. *Earth and Planetary Science Letters* **271**, 311–325.

Lissenberg, C. J. & MacLeod, C. J. (2016). A reactive porous flow control on mid-ocean ridge magmatic evolution. *Journal of Petrology* **57**, 2195–2220.

Lissenberg, C. J., MacLeod, C. J., Howard, K. A. & Godard, M. (2013). Pervasive reactive melt migration through fast-spreading lower oceanic crust (Hess Deep, equatorial Pacific Ocean). *Earth and Planetary Science Letters*. Elsevier **361**, 436–447.

Lissenberg, C. J., Riou, M., MacLeod, C. J., Bowring, S. A. & Shimizu, N. (2015). Crystallization depth beneath an oceanic detachment fault (ODP Hole 923A, Mid-Atlantic Ridge). *Geochemistry, Geophysics, Geosystems* **17**, 162–180.

Lissenberg, J. C., MacLeod, C. J. & Bennett, E. N. (2019). Consequences of a crystal mush-dominated magma plumbing system: A mid-ocean ridge perspective. *Philosophical Transactions of the Royal Society A: Mathematical, Physical and Engineering Sciences* **377**.

MacLeod, C. J. & Yaouancq, G. (2000). A fossil melt lens in the Oman ophiolite: Implications for magma chamber processes at fast spreading ridges. *Earth and Planetary Science Letters* **176**, 357–373.

ORIGINAL UNEDITED MANUSCRIPT

Downloaded from https://academic.oup.com/petrology/advance-article/doi/10.1093/petrology/egad005/6998539 by guest on 13 February 2023

966 Magee, C. *et al.* (2018). Magma plumbing systems: A geophysical perspective. *Journal of*
967 *Petrology* **59**, 1217–1251.
968 Mainprice, D. (1997). Modelling the anisotropic seismic properties of partially molten rocks
969 found at mid-ocean ridges. **279**, 161–179.
970 Mckenzie, D. (1984). The generation and compactation of partially molten rock. *Journal of*
971 *Petrology* **25**, 713–765.
972 Meurer, W. P. & Boudreau, A. E. (1989a). Compaction of Igneous Cumulates Part I:
973 Geochemical Consequences For Cumulates and Liquid Fractionation Trends. *The*
974 *Journal of Geology* **106**, 281–292.
975 Meurer, W. P. & Boudreau, A. E. (1989b). Compaction of Igneous Cumulates Part II:
976 Compaction and the Development of Igneous Foliations. *The Journal of Geology* **106**,
977 293–304.
978 Meyer, P. S., Dick, H. J. B. & Thompson, G. (1989). Cumulate gabbros from the Southwest
979 Indian Ridge, 54°S-7°16' E: implications for magmatic processes at a slow spreading
980 ridge. *Contributions to Mineralogy and Petrology* **103**, 44–63.
981 Namur, O. & Charlier, B. (2012). Efficiency of compaction and compositional convection
982 during mafic crystal mush solidification: The Sept Iles layered intrusion, Canada.
983 *Contributions to Mineralogy and Petrology* **163**, 1049–1068.
984 Namur, O., Humphreys, M. C. S. & Holness, M. B. (2013). Lateral reactive infiltration in
985 avertical gabbroic crystal mush, skaergaard intrusion, east greenland. *Journal of*
986 *Petrology* **54**, 985–1016.
987 Neave, D. A., Namur, O., Shorttle, O. & Holtz, F. (2019). Magmatic evolution biases basaltic
988 records of mantle chemistry towards melts from recycled sources. *Earth and Planetary*
989 *Science Letters*. Elsevier B.V. **520**, 199–211.
990 O'Driscoll, B., Emeleus, C. H., Donaldson, C. H. & Daly, J. S. (2010). Cr-spinel seam

ORIGINAL UNEDITED MANUSCRIPT

Downloaded from https://academic.oup.com/petrology/advance-article/doi/10.1093/petrology/egad005/6998539 by guest on 13 February 2023

991 petrogenesis in the rum layered suite, NWScotland: Cumulate assimilation and in situ
992 crystallization in a deforming crystal mush. *Journal of Petrology* **51**, 1171–1201.
993 O'Neill, H. S. C. & Jenner, F. E. (2012). The global pattern of trace-element distributions in
994 ocean floor basalts. *Nature*. Nature Publishing Group **491**, 698–704.
995 O'Neill, H. S. C. & Jenner, F. E. (2016). Causes of the compositional variability among ocean
996 floor basalts. *Journal of Petrology* **57**, 2163–2194.
997 Paulatto, M., Hooft, E. E. E., Chrapkiewicz, K., Heath, B., Toomey, D. R. & Morgan, J. V
998 (2022). Advances in seismic imaging of magma and crystal mush. 1–31.
999 Perugini, D. & Poli, G. (2005). Viscous fingering during replenishment of felsic magma
1000 chambers by continuous inputs of mafic magmas: Field evidence and fluid-mechanics
1001 experiments. *Geology* **33**, 5–8.
1002 Picard, D., Arbaret, L., Pichavant, M., Champallier, R. & Launeau, P. (2011). Rheology and
1003 microstructure of experimentally deformed plagioclase suspensions. *Geology* **39**, 747–
1004 750.
1005 Rannou, E., Caroff, M. & Cordier, C. (2006). A geochemical approach to model periodically
1006 replenished magma chambers: Does oscillatory supply account for the magmatic
1007 evolution of EPR 17-19°S? *Geochimica et Cosmochimica Acta* **70**, 4783–4796.
1008 Ross, D. K. & Elthon, D. (1997). Cumulus and postcumulus crystallization in the oceanic
1009 crust: major- and trace-element geochemistry of Leg 153 gabbroic rocks. *Proceedings of*
1010 *the Ocean Drilling Program, Scientific Results* **153**, 333–353.
1011 Rubin, K. H., Sinton, J. M., MacLennan, J. & Hellebrand, E. (2009). Magmatic filtering of
1012 mantle compositions at mid-ocean-ridge volcanoes. *Nature Geoscience*. Nature
1013 Publishing Group **2**, 321–328.
1014 Sanfilippo, A., Macleod, C. J., Tribuzio, R., Lissenberg, C. J. & Zanetti, A. (2020). Early-
1015 Stage Melt-Rock Reaction in a Cooling Crystal Mush Beneath a (IODP Hole U1473A ,

ORIGINAL UNEDITED MANUSCRIPT

Downloaded from https://academic.oup.com/petrology/advance-article/doi/10.1093/petrology/egad005/6998539 by guest on 13 February 2023

Atlantis Bank , Southwest Indian Ridge). *Frontiers in Earth Science* **8**, 1–21.

Sanfilippo, A. & Tribuzio, R. (2013). Building of the deepest crust at a fossil slow-spreading centre (Pineto gabbroic sequence, Alpine Jurassic ophiolites). *Contributions to Mineralogy and Petrology* **165**, 705–721.

Sanfilippo, A., Tribuzio, R., Tiepolo, M. & Berno, D. (2015). Reactive flow as dominant evolution process in the lowermost oceanic crust: evidence from olivine of the Pineto ophiolite (Corsica). *Contributions to Mineralogy and Petrology*. Springer Berlin Heidelberg **170**, 1–12.

Schaen, A. J., Schoene, B., Dufek, J., Singer, B. S., Eddy, M. P., Jicha, B. R. & Cottle, J. M. (2021). Transient rhyolite melt extraction to produce a shallow granitic pluton. *Science Advances* **7**, eabf0604.

Seropian, G., Kennedy, B. M., Walter, T. R., Ichihara, M. & Jolly, A. D. (2021). A review framework of how earthquakes trigger volcanic eruptions. *Nature Communications*. Springer US **12**, 1–13.

Shimizu, K., Saal, A. E., Hauri, E. H., Perfit, M. R. & Hékinian, R. (2019). Evaluating the roles of melt-rock interaction and partial degassing on the CO2/Ba ratios of MORB: Implications for the CO2 budget in the Earth's depleted upper mantle. *Geochimica et Cosmochimica Acta* **260**, 29–48.

Singh, S. C., Kent, G. M., Collier, J. S., Harding, A. J. & Orcutt, J. A. (1998). Melt to mush variations in crustal magma properties along the ridge crest at the southern East Pacific Rise. *Nature* **394**, 874–878.

Sinton, J. M. & Detrick, R. S. (1992). Mid-ocean ridge magma chambers. *Journal of Geophysical Research* **97**, 197–216.

Solano, J. M. S., Jackson, M. D., Sparks, R. S. J. & Blundy, J. (2014). Evolution of major and trace element composition during melt migration through crystalline mush: Implications

ORIGINAL UNEDITED MANUSCRIPT

Downloaded from https://academic.oup.com/petrology/advance-article/doi/10.1093/petrology/egad005/6998539 by guest on 13 February 2023

for chemical differentiation in the crust. *American Journal of Science* **314**, 895–939.

Sparks, R. S. J., Annen, C., Blundy, J. D., Cashman, K. V., Rust, A. C. & Jackson, M. D. (2019). Formation and dynamics of magma reservoirs. *Philosophical Transactions of the Royal Society A: Mathematical, Physical and Engineering Sciences* **377**.

Spera, F. J. & Bohrson, W. A. (2004). Open-system magma chamber evolution: An energy-constrained geochemical model incorporating the effects of concurrent eruption, recharge, variable assimilation and fractional crystallization (EC-E′RAχ FC). *Journal of Petrology* **45**, 2459–2480.

Tait, S., Jaupart, C. & Vergniolle, S. (1989). Pressure, gas content and eruption periodicity of a shallow, crystallising magma chamber. *Earth and Planetary Science Letters* **92**, 107–123.

Tait, S. R., Huppert, H. E. & Sparks, R. S. J. (1984). The role of compositional convection in the formation of adcumulate rocks. *Lithos* **17**, 139–146.

Till, C. B., Vazquez, J. A. & Boyce, J. W. (2015). Months between rejuvenation and volcanic eruption at Yellowstone caldera, Wyoming. *Geology* **43**, 695–698.

Toplis, M. J., Brown, W. L. & Pupier, E. (2008). Plagioclase in the Skaergaard intrusion. Part 1: Core and rim compositions in the layered series. *Contributions to Mineralogy and Petrology* **155**, 329–340.

Troll, V. R., Mattsson, T., Upton, B. G. J., Emeleus, C. H., Donaldson, C. H., Meyer, R., Weis, F., Dahrén, B. & Heimdal, T. H. (2020). Fault-Controlled Magma Ascent Recorded in the Central Series of the Rum Layered Intrusion, NW Scotland. *Journal of Petrology* **61**.

Vigneresse, J. L., Barbey, P. & Cuney, M. (1996). Rheological transitions during partial melting and crystallization with application to felsic magma segregation and transfer. *Journal of Petrology* **37**, 1579–1600.

ORIGINAL UNEDITED MANUSCRIPT

Downloaded from https://academic.oup.com/petrology/advance-article/doi/10.1093/petrology/egad005/6998539 by guest on 13 February 2023

Voshage, H., Hofmann, A. W., Mazzucchelli, M., Rivalenti, G., Sinigoi, S., Raczek, I. & Demarchi, G. (1990). Isotopic evidence from the Ivrea Zone for a hybrid lower crust formed by magmatic underplating. *Nature* **347**, 731–736.

Wager, L. R., Brown, G. M. & Wadsworth, W. J. (1960). Types of Igneous Cumulates. *Journal of Petrology* **1**, 73–85.

Whitehead, J. A. & Helfrich, K. R. (1991). Instability of flow with temperature-dependent viscosity: A model of magma dynamics. *Journal of Geophysical Research: Solid Earth* **96**, 4145–4155.

Woods, A. W. & Cardoso, S. S. S. (1997). Triggering basaltic volcanic eruptions by bubble-melt separation. *Nature* **385**, 518–520.

Xing, C. M., Wang, C. Y., Charlier, B. & Namur, O. (2022). Ubiquitous dendritic olivine constructs initial crystal framework of mafic magma chamber. *Earth and Planetary Science Letters*. Elsevier B.V. **594**, 117710.

Yang, A. Y., Wang, C., Liang, Y. & Lissenberg, C. J. (2019). Reaction between MORB magma and lower oceanic crust: An experimental study. *Geochemistry Geophysics Geosystems*.

Zandt, G., Leidig, M., Chmielowski, J., Baumont, D. & Yuan, X. (2003). Seismic detection and characterization of the Altiplano-Puna magma body, Central Andes. *Pure and Applied Geophysics* **160**, 789–807.

Zhang, W.-Q., Dick, H. J. B., Liu, C.-Z., Lin, Y.-Z. & Angeloni, L. M. (2021). MORB Melt Transport Through Atlantis Bank Oceanic Batholith (SW Indian Ridge). *Journal of Petrology*.

Zhang, W.-Q., Liu, C.-Z. & Dick, H. J. B. (2020). Evidence for Multi-stage Melt Transport in the Lower Ocean Crust: the Atlantis Bank Gabbroic Massif (IODP Hole U1473A, SW Indian Ridge). *Journal of Petrology* **61**.

ORIGINAL UNEDITED MANUSCRIPT

Downloaded from https://academic.oup.com/petrology/advance-article/doi/10.1093/petrology/egad005/6998539 by guest on 13 February 2023

1091 Box 1. Definitions

Magma or igneous reservoir:
Structure that comprises a porous and permeable framework of crystals (mush) with melt present in the pore space (low-melt-fraction mush reservoir from Jackson *et al.*, 2018).

Magma chamber:
Structure that stores at depth melts liquid-rich regions (high-melt-fraction mush reservoir from Jackson *et al.*, 2018).

Magma:
System of melt containing crystals (and gases) where the crystal load forms a discontinuous or unlocked framework that allows magma migration (Sparks *et al.*, 2019).

Mush:
"Any system of crystals and melt (and gases) in which the crystals form a continuous framework through which melt is distributed" (Cashman *et al.*, 2017).

Melt-rock reaction:
Reaction between a rock and melts in contact.

Melt-mush reaction:
Reaction between preexisting cumulate minerals from an active mush and melts in contact.

Reactive porous flow (RPF):
Series of reactions of a melt with the rock or mush through which it is percolating.

Differentiation:
Any process whereby a magma, without foreign contamination, forms either a mass of rock that has different compositions in different parts or separate masses that differ from one another in composition (Bowen 1915).

Assimilation-Fractional Crystallization:
Model considering the evolution of a magma by concurrent assimilation of lithologies and differentiation by fractional crystallization (Bowen, 1928; DePaolo, 1981).

Trapped melt crystallization:
Extreme differentiation of residual interstitial melt trapped within the porosity remnant of a rock by fractional crystallization (Meyer *et al.*, 1989; Bédard, 1994; Sanfilippo *et al.*, 2020).

In situ crystallization:
Crystallization of a magma at the magma chamber margins with various fractions of the interstitial melt of the mush boundary layer returning to the main magma body (Langmuir, 1989).

ORIGINAL UNEDITED MANUSCRIPT

Downloaded from https://academic.oup.com/petrology/advance-article/doi/10.1093/petrology/egad005/6998539 by guest on 13 February 2023

1092 Table 1A. Summary of the main geochemical and textural evidence for the occurrence of RPF in natural mid-
1093 ocean ridge and other crustal magmatic systems.

MOR systems	Studied area	Sample type	Geochemical evidence	Textural evidence
Coogan et al. (2000)	Kane Megamullion (MAR)	Poikilitic and brown-pyroxene gabbros	Zoned Cpx crystals with enrichments in Zr relative to REE	Equidimensional Pl with interdigitated grain boundaries in Cpx oikocrysts
Kvassnes (2003)	Atlantis Bank OCC (SWIR)	Clinopyroxenes from ODP Hole 735B gabbros	Increasing LREE/HREE ratios in augites with fractionation	-
Gao et al. (2007a)	Atlantis Bank OCC (SWIR)	Clinopyroxene from an olivine gabbro	Profiles in TEs in a Cpx grain (strong enrichments and fractionation between LREE and HREE towards the grain boundary)	-
Lissenberg & Dick (2008)	Kane Megamullion (MAR)	MORB	High-Mg# low-pressure Cpx with high Cr2O3 or high TiO2 contents	Crosscutting Cpx oikocrysts defining bands, enclosing Pl chadacrysts with irregularly curved grain boundaries (resorbed)
Lissenberg et al. (2013)	Hess Deep (EPR)	Gabbroic rocks	Large Pl An range for given Cpx Mg#, poor correlation between Cpx Mg# and TiO_2 and Cr_2O_3, enrichment and fractionation of incompatible TEs in Cpx, TEs	Dissolution fronts in Pl (An maps)

ORIGINAL UNEDITED MANUSCRIPT

Downloaded from https://academic.oup.com/petrology/advance-article/doi/10.1093/petrology/egad005/6998539 by guest on 13 February 2023

			disequilibrium between Ol, Pl and Cpx	
Leuthold et al. (2018)	Kane Megamullion (MAR)	Poikilitic gabbro and troctolite	Complex Cr, Ti, REE, Zr and Y zoning in coarse-grained Cpx oikocrysts	Large Cpx oikocrysts with resorption textures between zoned areas, Pl chadacrysts resorption textures
Zhang et al. (2020)	Atlantis Bank OCC (SWIR)	Olivine gabbros and oxide gabbros	Mineral HFSE/REE fractionations	Irregular contacts between Cpx oikocrysts and Pl chadacryst, resorbed Ol textures against Pl grains, corroded Ol chadacrysts in Pl or Cpx
Boulanger et al. (2020)	Atlantis Bank OCC (SWIR)	Troctolites, olivine gabbros, gabbros	High-Mg# and TiO_2 Cpx, decoupling between major and trace elements in Pl and Cpx, LREE/HREE fractionation of Pl	Cpx intergrowths, Cpx symplectite, complex Pl zoning, discordant Pl twins on irregular grain boundaries, rounded (resorbed) Ol grains
Sanfilippo et al. (2020)	Atlantis Bank OCC (SWIR)	Olivine gabbro	TEs zoning in Pl and Cpx, progressive fractionation betwen LREE and HREE towards grain boundaries of Pl and Cpx grains	Ox-rich gabbro patches and veinlets crosscutting the primitive Ol gabbros with resorbed Pl core relicts
Ferrando et al. (2021a)	Atlantis Bank OCC (SWIR)	Olivine gabbros	Pl and Cpx chemical zoning, LREE/HREE fractionation, TEs enrichment in rims	Pl grains (+/- chadacrysts) with lobate grain boundaries against Cpx, Ol with corroded contacts against Cpx or Pl
Boulanger et al.	Atlantis Bank OCC (SWIR)	Layered olivine gabbros	Corroded grain boundaries or	REE and TiO2 enrichment

ORIGINAL UNEDITED MANUSCRIPT

Downloaded from https://academic.oup.com/petrology/advance-article/doi/10.1093/petrology/egad005/6998539 by guest on 13 February 2023

(2021)			rounded grains of Ol, Cpx intergrowths, locally resorbed Pl and overgrown Cpx grain boundaries	in Cpx compared to an evolution by FC, LREE/HREE fractionation in Cpx
Other systems	**Studied area**	**Sample type**	**Geochemical evidence**	**Textural evidence**
Namur et al. (2013)	Skaergaard (East Greenland)	Inner Banded Division of the Marginal Border Series	-	(Colloform banding at intrusion margins)
Leuthold et al. (2014)	Rum Layered Intrusion (Scotland)	Allivalites	Cr and Al zoning in poikilitic Cpx	Troctolite replacement by anorthosite, complex zoning of poikilitic Cpx grains with dissolution evidence
Bouihol et al. (2015)	Sapat Complex (Pakistan)	Dunite and pyroxenites	-	Hornblende replacing Cpx textures, Opx replacing and Hbl replacing Ol textures, structural organization of lithologies
Cooper et al. (2016)	Martinique (France)	Plutonic xenoliths	Amp and Cpx variability in incompatible trace element signatures, REE enrichments in amphiboles with flat REE profiles	Reacted Pl rims, two generations of Amph (early and late appearance), interstitial amphiboles associated with Cpx
Hepworth et al. (2020)	Rum Layered Intrusion (Scotland)	Cpx-rich wherlites	-	Large poikilitic Cpx, zoned Cpx oikocryst with small rounded Ol chadacrysts
Gleeson et al. (2021)	Isla Floreana (Ecuador)	Wehrlites, dunites and gabbro xenoliths	TE disequilibria (cumulus phases - erupted melts) LREE fractionation	Poikilitic Cpx and lack of evidence for trapped melt crystallization

ORIGINAL UNEDITED MANUSCRIPT

Downloaded from https://academic.oup.com/petrology/advance-article/doi/10.1093/petrology/egad005/6998539 by guest on 13 February 2023

			(La/Sm, Ce/Y) in Cpx xenoliths	
Xing et al. (2022)	Sept Iles layered intrusion (Canada)	Ol primocrysts	P zoning patterns in Ol	Dendritic, hopper and sector patterns of high-P zones corroded by P-poor Ol domains

ORIGINAL UNEDITED MANUSCRIPT

Downloaded from https://academic.oup.com/petrology/advance-article/doi/10.1093/petrology/egad005/6998539 by guest on 13 February 2023

1131 Table 1B. Summary of the main reactions characteristic of RPF in natural mid-ocean ridge and
1132 other crustal magmatic systems and associated numerical models parameters.

MOR systems	**Studied area**	**Assimilated material**	**Reactive melt**	**Reaction(s)**	Model	r = Ma/Mc
Coogan et al. (2000)	Kane Megamullion (MAR)	Primitive clinopyroxene	-	Cpx + melt1 -> Cpx + melt2	AFC (DePaolo 1981)	0,7 - 0,8 - 0,9
Kvassnes (2004)	Atlantis Bank OCC (SWIR)	Olivine gabbro	-	Ol_{15} + Pl_{50} + Cpx_{35} + melt1 -> Ol + Pl + Cpx + melt2	AFC (DePaolo 1981)	0,5 - 0,8 - 0,9
Gao et al. (2007a)	Atlantis Bank OCC (SWIR)	Primitive clinopyroxene	Primitive melt (Cpx core equilibrium melt)	Cpx + melt1 -> Pl_{100-60} + Cpx_{0-40} + melt2	AFC (DePaolo 1981)	[0,5 ; 0,9]
Lissenberg & Dick (2008)	Kane Megamullion (MAR)	Troctolitic mush	Primitive MORB and more evolved MORB	$Ol_{86/80/67}$ + $Pl_{14/20/33}$ + melt1 -> Pl_{56} + Cpx_{44} + melt2	Major element mass balance	2 - 0,75
Lissenberg et al. (2013)	Hess Deep (EPR)	Gabbroic mush	-	$Ol_{[0;60]}$ + $Pl_{[0;80]}$ + $Cpx_{[0;100]}$ + melt1 -> $Ol_{[10;50]}$ + $Pl_{[10;70]}$ + $Cpx_{[10;70]}$ + melt2	AFC (DePaolo 1981)	[0,75; 0,95]
Leuthold et al. (2018)	Kane Megamullion (MAR)	Gabbroic protolith	Primitive mantle-derived melt	Ol + Pl + Cpx + melt1 -> Ol + Pl + Cpx + melt2 Ol + Pl + Cpx + melt3 -> Ol + Pl + Cpx + Sp + melt4	MASH (Hildreth & Moorbath (1988)	-
Zhang et al.	Atlantis Bank OCC	Gabbroic mush	Primitive melt (Cpx	Ol_{15} + Pl_{50} + Cpx_{35} +	AFC (DePaolo	[0,6; 0,9]

ORIGINAL UNEDITED MANUSCRIPT

Downloaded from https://academic.oup.com/petrology/advance-article/doi/10.1093/petrology/egad005/6998539 by guest on 13 February 2023

(2020)	(SWIR)		equilibrium melt)	melt1 -> Ol_6 + Pl_{56} + Cpx_{38} + Opx_1 + melt2 Ol_{15} + Pl_{50} + Cpx_{35} + melt1 -> Ol_6 + Pl_{56} + Cpx_{38} + Opx_1 + $Ilm_{0,6/1,4}$ + melt2	1981) AFC (DePaolo 1981)	[0,6; 0,9]
Boulanger et al. (2020)	Atlantis Bank OCC (SWIR)	Troctolitic mush	Primitive MORB (SWIR) and reactive melts	Ol_{45} + Pl_{55} + melt1 -> Pl100 + melt2 Ol_{45} + Pl_{55} + melt1 -> Ol_5 + Pl_{50} + Cpx_{45} + melt2 Ol_{45} + Pl_{55} + melt1 -> Pl_{55} + Cpx_{45}	AFC (DePaolo 1981) AFC (DePaolo 1981) AFC (DePaolo 1981)	[0,9; 0,99] [0,5; 0,9] [0,6; 0,99]
Sanfilippo et al. (2020)	Atlantis Bank OCC (SWIR)	Gabbroic mush	Primitive melt (Cpx ad Pl equilibrium melt)	Ol_{10} + Pl_{50} + Cpx_{40} + melt1 -> Pl_{60} + Cpx_{40} + melt2	AFC (DePaolo 1981)	0,99
Ferrando et al. (2021a)	Atlantis Bank OCC (SWIR)	Troctolitic mush and gabbroic mush	N-MORB (SWIR) and reactive melts	Ol_{40} + Pl_{60} + melt1 -> Ol_{10} + Cpx_{30} + melt2 Ol + Pl + Cpx + melt2 -> Pl + Cpx + melt3	AFC (DePaolo 1981) AFC (DePaolo 1981)	[0,6; 0,85] [0,6; 0,85]
Boulanger et al. (2021)	Atlantis Bank OCC (SWIR)	Gabbroic mush	Primitive melt (intrusion and Pl equilibrium melt)	Ol_{11} + Pl_{50} + Cpx_{39} + melt1 -> Pl_{50} + Cpx_{50} + melt2	AFC (DePaolo 1981) Plate Model	[0,2; 0,85]

ORIGINAL UNEDITED MANUSCRIPT

Downloaded from https://academic.oup.com/petrology/advance-article/doi/10.1093/petrology/egad005/6998539 by guest on 13 February 2023

				$Pl_{40/30/20}$ + $Cpx_{60/70/80}$ + melt1 -> $Pl_{70/50}$ + $Cpx_{30/50}$ + melt2	(Vernières et al., 1997)	
Other systems	**Studied area**	**Assimilated material**	**Reactive melt**	**Reaction(s)**	**Model**	**r = Ma/Mc**
Namur et al. (2013)	Skaergaard (East Greenland)	Gabbroic crystal mush	Dry mafic silicate melt	Ol1 + Cpx1 + melt1 -> Ol2 + Cpx2 + melt2	-	-
Leuthold et al. (2014)	Rum LI (Scotland)	Gabbro pile	Differentiated picritic magma	-	-	-
Bouihol et al. (2015)	Sapat Complex (Pakistan)	Lower crustal metagabbro	Mantle basaltic melts	Cpx + melt1 -> Hbl + melt2, Ol+ melt3 -> Opx + Hbl + melt4	-	-
Cooper et al. (2016)	Martinique (France)	Mush with Cpx and early formed Amph	Water-rich Pl-undersaturated melts	Cpx + melt1 -> Amp + melt2	-	-
Hepworth et al. (2020)	Rum LI (Scotland)	Feldspathic peridotite protolith	Cpx-oversaturated melt	-	-	-
Gleeson et al. (2021)	Isla Floreana (Ecuador)	Ol-dominated mush	Cpx-saturated melts	Ol + melt1 -> Cpx + melt2	Zone refining (Harris, 1957)	-
Xing et al. (2022)	Sept Iles layered intrusion (Canada)	Early-formed Ol grains	Primary magma recharge(s)	-	-	-

ORIGINAL UNEDITED MANUSCRIPT

Downloaded from https://academic.oup.com/petrology/advance-article/doi/10.1093/petrology/egad005/6998539 by guest on 13 February 2023

1137 FIGURE 1. Cumulate geochemical signatures. Mean rare earth element (REE) compositions of
1138 oceanic plutonic rocks from (a) the mid-Atlantic ridge ('MAR'; Atlantis Massif, IODP Hole
1139 U1309D; from Godard *et al.*, 2009) and (b) the Southwest Indian Ridge ('SWIR'; Atlantis Bank,
1140 ODP Hole 735B; from Dick *et al.*, 2000). Elemental concentrations are normalized to a primary
1141 MORB magma, calculated as the melt formed after 10% fractional melting of the Depleted
1142 MORB Mantle following the procedure of Godard *et al.* (2009). MORB compositions are from
1143 the PetDB database (Aug. 2020) and Coogan *et al.* (2004). Plutonic rocks with REE contents
1144 lower than those of the primary MORB (normalized concentrations <1) display characteristic
1145 cumulate signatures (e.g., Eu enrichment, Supplementary Materials Table S1).
1146
1147 FIGURE 2. Petrographic evidence of reactive porous flow. Microphotographs (cross-polarized
1148 light), and chemical map (g) of oceanic plutonic samples presenting characteristic reactive
1149 textures. (a) Clinopyroxenes (Cpx) intergrowths in an olivine gabbro (ODP Hole 735B,
1150 Lissenberg et al., 2013). Scale bar: 1mm. (b) Rounded olivine (Ol) grains within a poikilitic
1151 anhedral Cpx (Erro Tobio troctolites, Borghini and Rampone, 2007). Scale bar: 0.5mm. (c)
1152 Partially resorbed plagioclase grains (Pl) in a poikilitic coarse grained Cpx (scale bar: 2.5mm)
1153 and (d) Ol with rounded resorbed shapes in contact with Pl and Cpx in olivine gabbros from
1154 IODP Hole U1473A (Ferrando et al., 2021b). Scale bar: 0.5mm. (e) Plagioclase dissolution
1155 textures in a poikilitic Cpx from the Kane Megamullion (Lissenberg and Dick, 2008). Scale bar:
1156 3mm. (f) Detailed thin section in ODP Hole 735B-91R-1 sample with numerous rounded olivine
1157 grains and plagioclase grains with irregular boundaries engulfed in cm-wide clinopyroxene
1158 oikocrysts (red grain boundaries). Scale bar: 1 cm. (Boulanger et al., 2020). (g) Anorthite (molar
1159 fraction An = Ca/(Ca+Na+K)x100) map showing dissolution fronts in Pl (Hess Deep gabbro,
1160 Lissenberg et al., 2013). Scale bar: 0.5mm. (h) Pl grain with resorbed grain boundary included in

ORIGINAL UNEDITED MANUSCRIPT

Downloaded from https://academic.oup.com/petrology/advance-article/doi/10.1093/petrology/egad005/6998539 by guest on 13 February 2023

a Cpx crystal presenting symplectite textures, (i) Pl grain with complex zoning and irregular grain boundaries, (j) Pl with irregular grain boundaries crosscutting twins and Cpx intergrowths and (k) rounded-shape Ol crystals and plagioclase presenting complex zoning from ODP Hole 735B (Boulanger et al., 2020). Scale bars: 0.5mm. (l) Cpx intergrowths, small resorbed Pl chadacrysts in a large Cpx (m) and Pl (n) crystal, and (o) round-shaped Ol chadacryst within a larger Cpx (IODP Hole U1473A, Boulanger et al., 2021). Scale bars: 0.5mm. (p) Pl grains enclosed by a large Cpx oikocryst with irregular contacts, (q) irregularly-shaped Ol with resorbed textures, (r) highly corroded small Ol grains enclosed by Cpx and Pl and (s) Pl grain with deformation twins and irregular contacts with surrounding minerals (IODP Hole U1473A, Zhang et al., 2020). Scale bars for (p), (q) and (r): 2mm. Scale bar for (s): 1mm.

FIGURE 3. Geochemical evidence for reactive porous flow and characteristics. (a) La_N/Sm_N ratios versus La_N analyzed in plagioclases from oceanic cumulates (olivine gabbros from ODP Hole 735B; Boulanger *et al.*, 2020), and expected composition of Pl after fractional crystallization (FC) and assimilation-fractional crystallization (AFC). Values normalized to the average primitive MORB composition in the Atlantis Bank area (MORBs from *Coogan et al., 2004*). Red and yellow trends: modeled plagioclase compositions after FC from two different parental melts (melts in equilibrium with plagioclases bearing the most primitive signatures from the Upper - red start - and Lower - yellow star - units of the section). Natural Pl compositions, FC and AFC models from Boulanger *et al.* (2020). (b) Summary of literature r values (the ratio of mass assimilated to that crystallized during AFC) obtained by fitting natural data with AFC models in oceanic plutonic sections where RPF has been quantified. r values are here compared to clinopyroxene Mg# of the studied oceanic sections (Coogan *et al.*, 2000; Kvassnes, 2004; Gao *et al.*, 2007; Boulanger *et al.*, 2020; Sanfilippo *et al.*, 2020; Zhang *et al.*, 2020, 2021; Ferrando *et*

ORIGINAL UNEDITED MANUSCRIPT

Downloaded from https://academic.oup.com/petrology/advance-article/doi/10.1093/petrology/egad005/6998539 by guest on 13 February 2023

1185 *al.*, 2021b). Values of r below 1 indicate preferential crystallization during reactive porous flow,
1186 whereas values above 1 indicate preferential assimilation. For additional r values from the
1187 literature, see Table 1.
1188
1189 FIGURE 4. Comparison of minerals and melt compositions obtained by theoretical models of
1190 AFC (*DePaolo, 1981*) with natural minerals and melt (MORB) compositions. The models
1191 presented in a given row of the figure consider crystallization of one single oceanic cumulate
1192 forming mineral, either Ol, Pl or Cpx. The models presented in a given column of the figure show
1193 the resulting compositions in either Pl, Cpx or melts after AFC. For each graph, assimilation of
1194 Ol (green lines), Pl (blue lines) or Cpx (red lines) are considered for different r = Ma/Mc ratios
1195 ranging from 0 (equivalent to fractional crystallization) to 0.99. Additional black lines correspond
1196 to pure assimilation modelled by mixing between the mineral composition (Ol, Pl or Cpx) and the
1197 composition of the melt used in the AFC models (yellow star). Natural Pl and Cpx compositions
1198 are from Lissenberg *et al.*, 2013 (L13), Lissenberg and MacLeod, 2016 (L&M16), Ferrando *et*
1199 *al.*, 2021b (F21), Boulanger *et al.*, 2021 (B21), Boulanger *et al.*, 2020 (B20) and Boulanger, 2020
1200 (this study). MORB melts from fast-spreading ridges (FSR) and slow-spreading ridges (SSR)
1201 from Gale *et al.* (2013). Input parameters of the AFC models available in Supplementary
1202 materials (Table S2).
1203
1204 FIGURE 5. Results of AFC thermodynamic models using the Magma Chamber Simulator
1205 (Bohrson et al., 2014). All results are given as equivalent mass (g). The initial mass of Magma is
1206 100 g for all models. (a) Amount of material from the *Mush* assimilated into the *Magma* and
1207 amount of material crystallized from the *Magma* during the AFC process. r = ratio between the
1208 total assimilated mass and the total crystallized mass. (b) Initial and final state of the *Mush* for

ORIGINAL UNEDITED MANUSCRIPT

Downloaded from https://academic.oup.com/petrology/advance-article/doi/10.1093/petrology/egad005/6998539 by guest on 13 February 2023

each AFC process modeled, after assimilation and crystallization. For more details, see **Thermodynamic feasibility test** and Supplementary Materials Table S3.

FIGURE 6. Simplified view of a mush where *melt flush* occurs. This figure shows the progressive removal of interstitial evolved melt (L_{n+1}) from the crystal matrix replaced by the primitive melt (L_n, *Magma* in the MCS models) that partially assimilates the minerals before crystallization of a new generation recording both the average more primitive character of the melt and textural and chemical evidence for RPF.

FIGURE 7. The *melt flush* process. Schematic diagram of the *melt flush* process, and a summary of the processes occurring during the formation of cumulate igneous rocks from a petrologic perspective. Continuous and cyclic replenishment refers to oscillatory melt replenishment cycles by melt intrusions that vary through time (see Boulanger *et al.*, 2020, for further details). RPF: reactive porous flow.

ORIGINAL UNEDITED MANUSCRIPT

Downloaded from https://academic.oup.com/petrology/advance-article/doi/10.1093/petrology/egad005/6998539 by guest on 13 February 2023

Fig. 1.

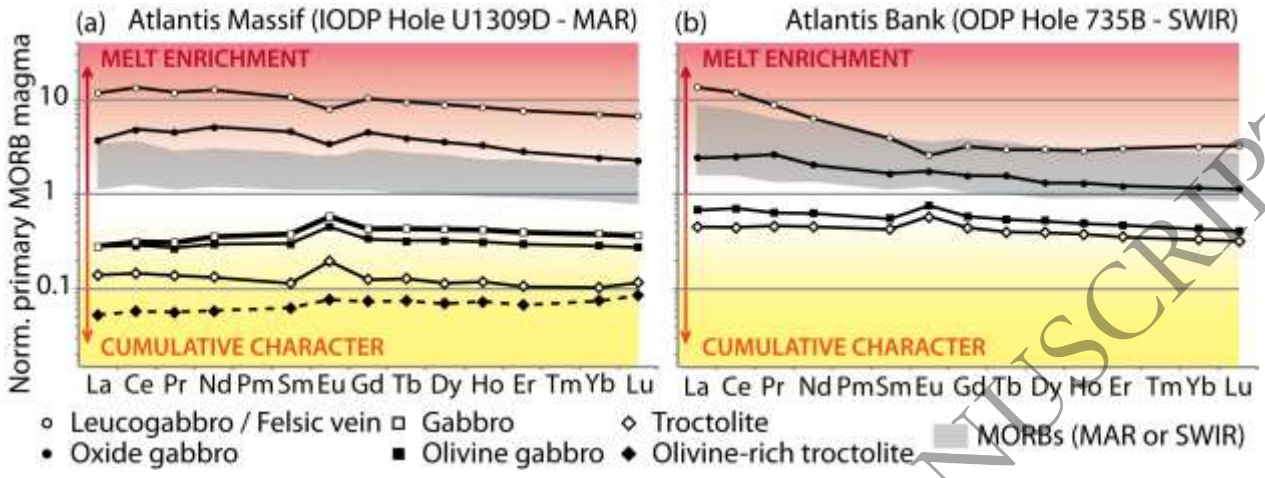

ORIGINAL UNEDITED MANUSCRIPT

Downloaded from https://academic.oup.com/petrology/advance-article/doi/10.1093/petrology/egad005/6998539 by guest on 13 February 2023

Fig. 2.

ORIGINAL UNEDITED MANUSCRIPT

Downloaded from https://academic.oup.com/petrology/advance-article/doi/10.1093/petrology/egad005/6998539 by guest on 13 February 2023

1275 **Fig. 3.**

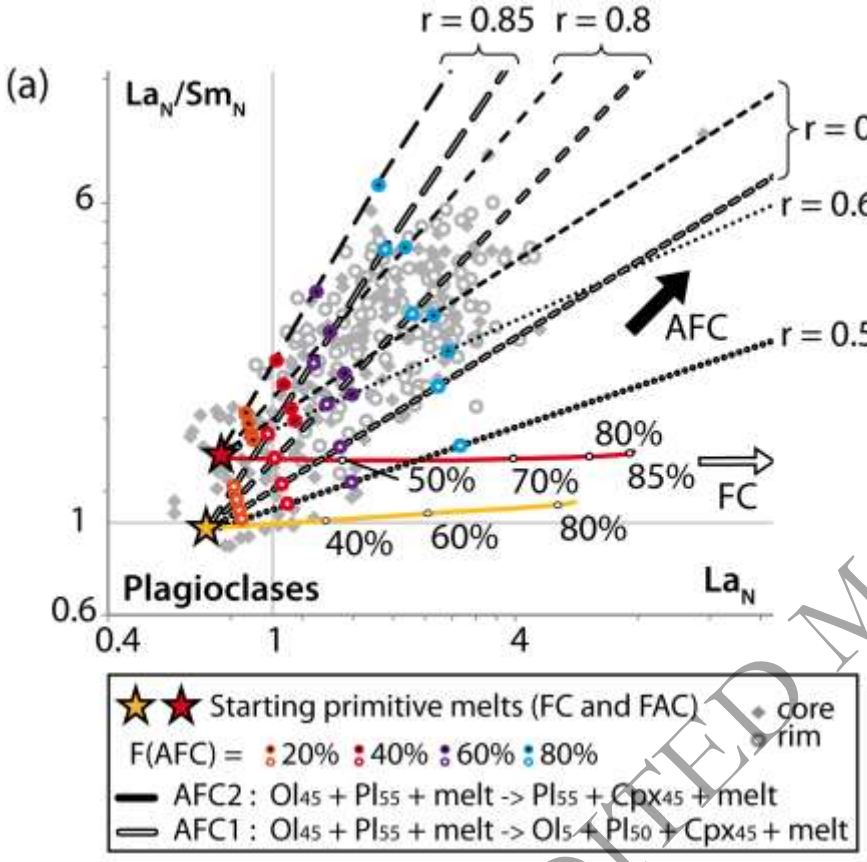

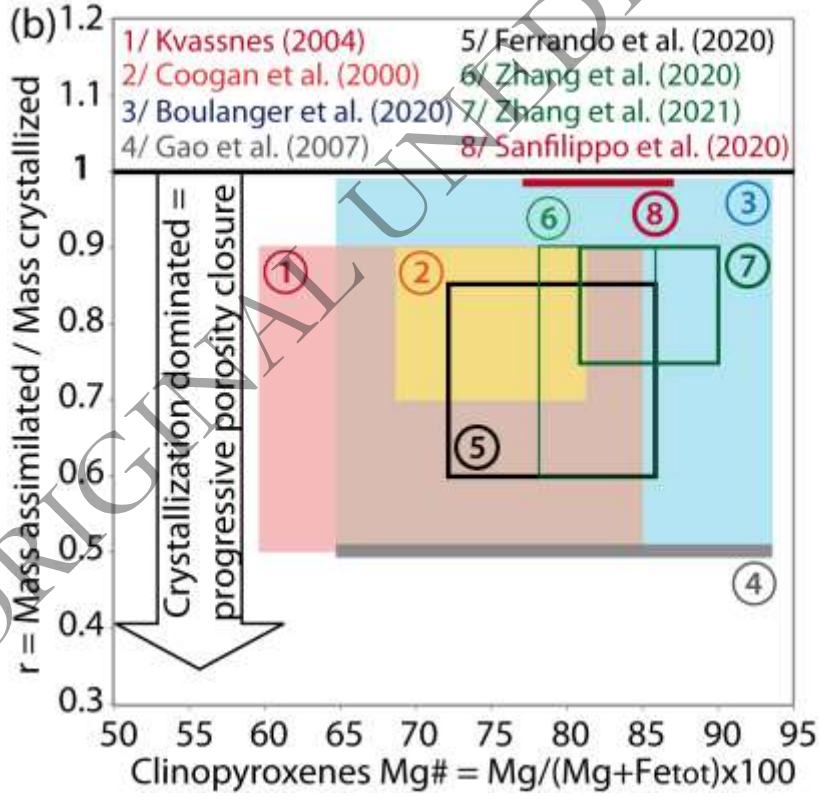

1276

ORIGINAL UNEDITED MANUSCRIPT

Downloaded from https://academic.oup.com/petrology/advance-article/doi/10.1093/petrology/egad005/6998539 by guest on 13 February 2023

Fig. 4.

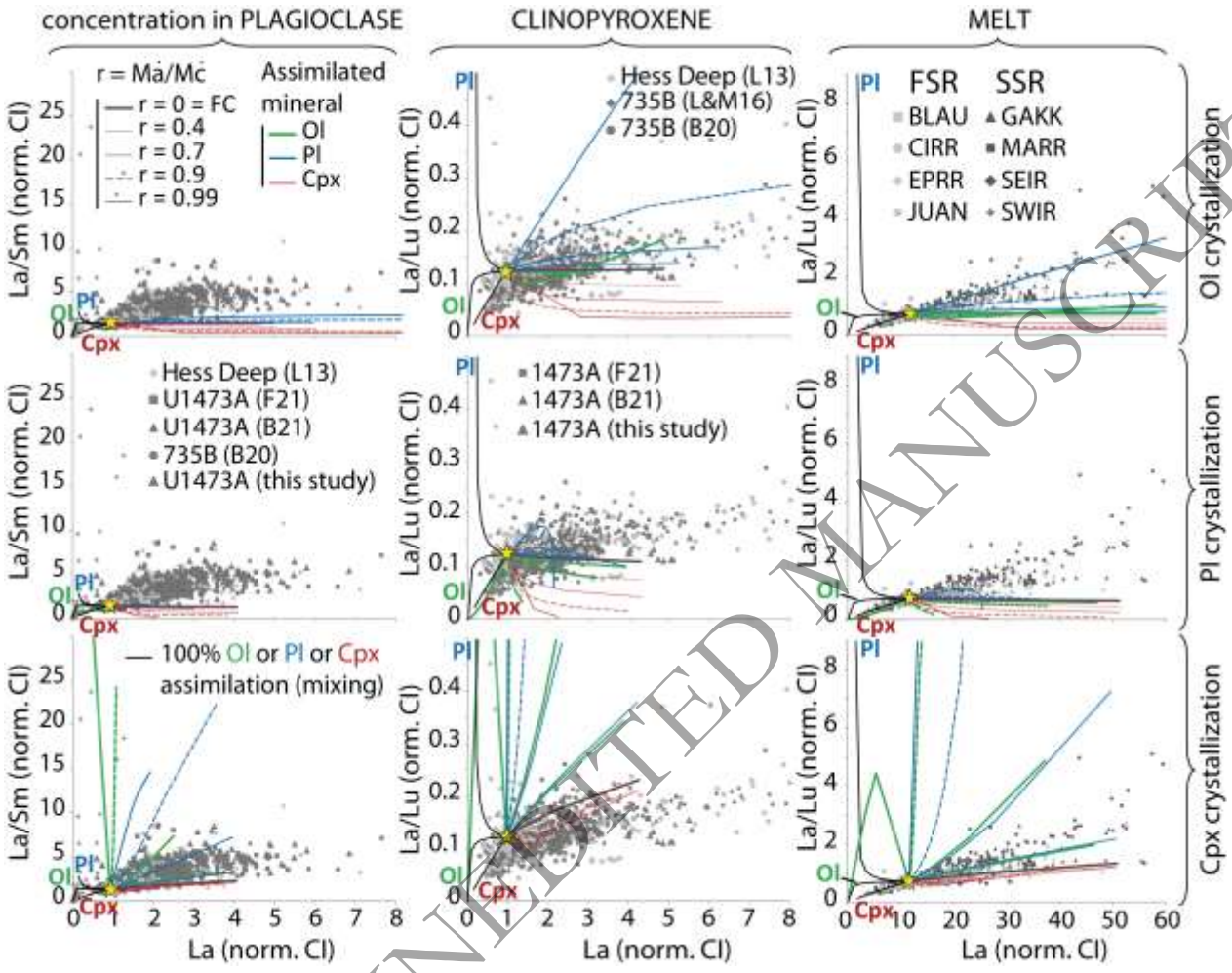

ORIGINAL UNEDITED MANUSCRIPT

Downloaded from https://academic.oup.com/petrology/advance-article/doi/10.1093/petrology/egad005/6998539 by guest on 13 February 2023

Fig. 5.

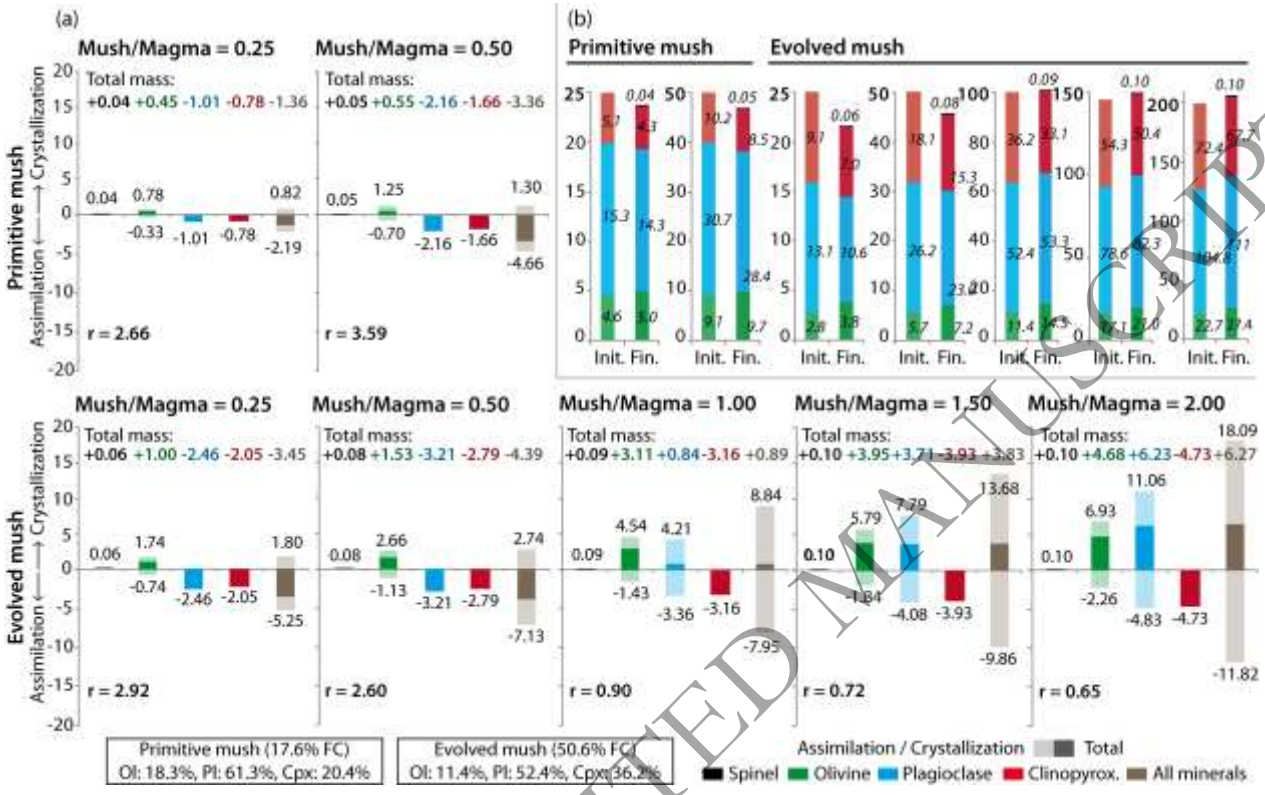

ORIGINAL UNEDITED MANUSCRIPT

Downloaded from https://academic.oup.com/petrology/advance-article/doi/10.1093/petrology/egad005/6998539 by guest on 13 February 2023

Fig. 6.

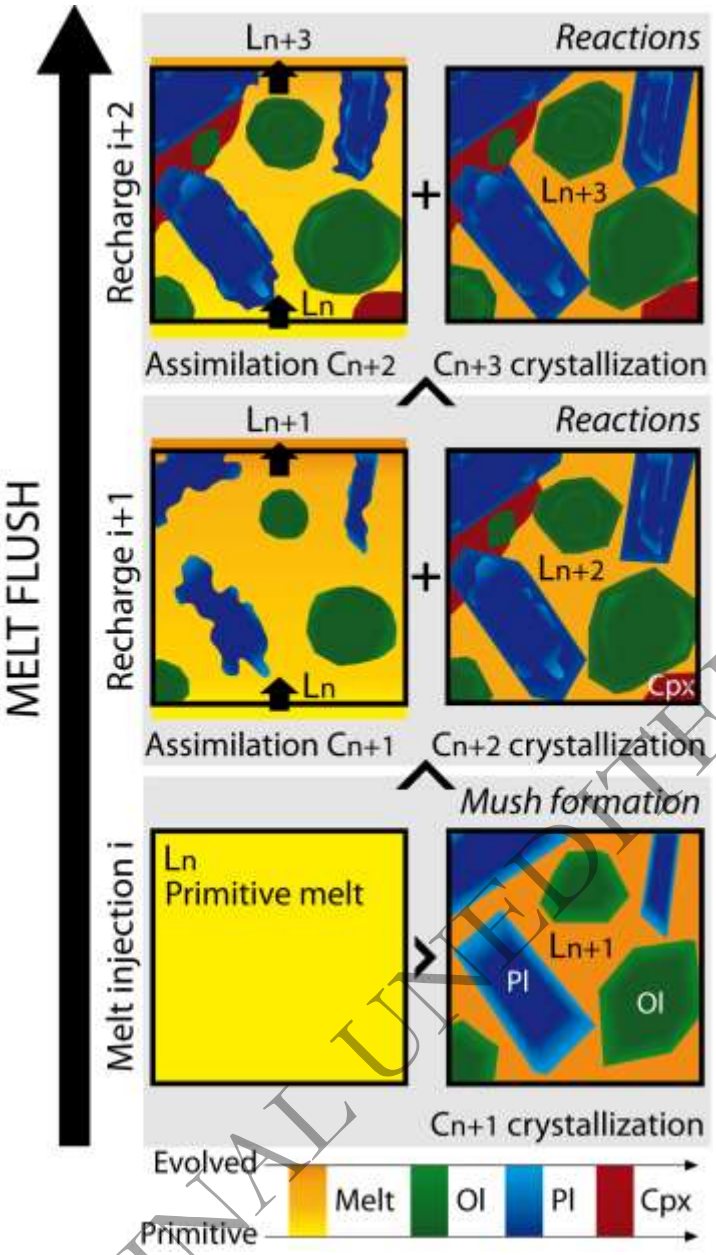

ORIGINAL UNEDITED MANUSCRIPT

Downloaded from https://academic.oup.com/petrology/advance-article/doi/10.1093/petrology/egad005/6998539 by guest on 13 February 2023

1338 **Fig. 7.**

1339

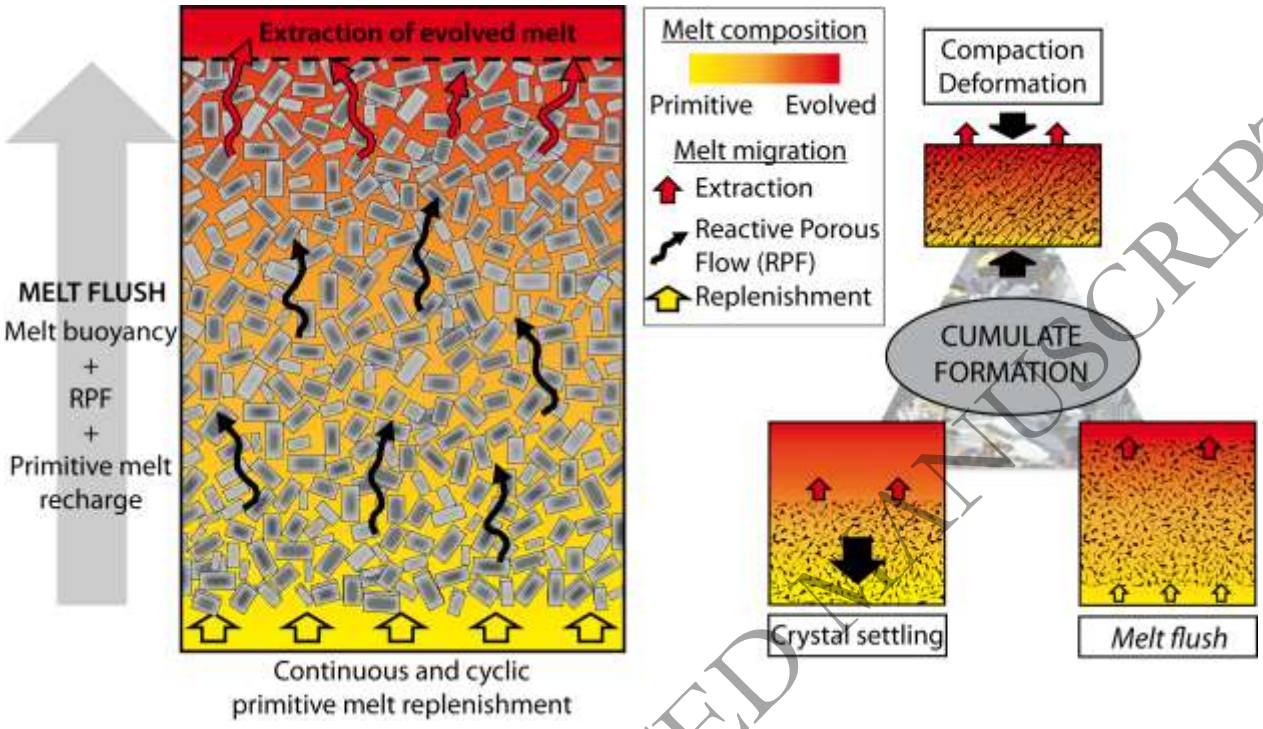

1340

ORIGINAL UNEDITED MANUSCRIPT

Downloaded from https://academic.oup.com/petrology/advance-article/doi/10.1093/petrology/egad005/6998539 by guest on 13 February 2023